Moment models for an axisymmetric inertial connement experiment and one dimensional numerical study

Xavier Blanc, Patricia Cargo, Tony Février, Gérald Samba

Moment models for an axisymmetric inertial confinement experiment and one dimensional numerical study

Xavier Blanc[1], Patricia Cargo[2], Tony Février[3], Gérald Samba[2]

[1]Université de Paris, CNRS, Sorbonne Université,
Laboratoire Jacques-Louis Lions (LJLL), F-75005 Paris,
xavier.blanc@u-paris.fr

[2]CEA, DAM, DIF, F-91297 Arpajon, France
patricia.cargo@cea.fr gerald.samba@cea.fr

[3]Institut Villebon Georges Charpak, Université Paris Sacalay,
Bâtiment 490, rue Hector Berlioz, F-91400 Orsay,
tony.fevrier@universite-paris-sacalay.fr

January 31, 2022

Abstract

In Inertial Confinement Fusion (ICF) experiments, radiation is well described by a kinetic model (radiative transfer equation). This model is usually too expensive to be used in numerical simulations of such phenomena. Hence, approximations are used. A common one is to use a moment model, in which the radiative transfer equation is replaced by its first and second order (in velocity) moments, together with a closure assumption. In this article, we propose a closure for 2D and 3D geometries, which are extensions of a one-dimensional radially symmetric model called P_1'. This model has proved to be very accurate in the study of ICF, which makes the models we propose promising in this respect. The closure is based on the fact that the model should, if possible, reproduce the exact solutions of radiative transfer equation in vacuum. We also design a numerical scheme for the radially symmetric case. This scheme is well-balanced and satisfies the diffusion limit of the model. This scheme is validated by various numerical tests.

Contents

Introduction

Inertial confinement fusion aims at reaching thermonuclear fusion in a laboratory using high energy laser beams. In such an experiment, a small plastic ball (the target) filled with hydrogen (deuterium and tritium) is heated up. Doing so, the external layers of the target are dilated. Conservation of momentum implies that the inner layers are contracted, so that the pressure and temperature of the combustible are increased, hopefully reaching values allowing for fusion reactions. In order to heat up the target, mainly two approaches are used: the direct one, in which the laser beams are pointed directly towards the target, and the indirect one, in which the target is inserted inside a small cavity (hohlraum) with golden walls. These walls are heated up by laser beams, and emit X-rays towards the target (see Figure 1). The advantage of the first approach is that the laser energy is more directly transmitted to the target, at the price of being highly anisotropic. On the other hand, indirect approach gives a more isotropic energy flux on the target boundary, while an important part of the laser energy is wasted in heating up the hohlraum walls.

Inertial confinement fusion experiments involve many different physical phenomena such as laser-plasma interaction, radiative transfer, neutronics and plasma hydrodynamics. This contribution focuses on the radiative transfer, which is of particular importance in the indirect approach. A good approximation in this case is that of a kinetic description of a photon gas: the radiative intensity [8] is a distribution function $I = I(t, \mathbf{x}, \mathbf{\Omega})$. It depends on time $t \in \mathbb{R}$, on space position $\mathbf{x} \in \mathbb{R}^3$ and the propagation direction $\mathbf{\Omega} \in \mathcal{S}^2$ where $\mathcal{S}^2$ is the unit sphere of $\mathbb{R}^3$. The velocity of photons is the speed of light c. For the sake of simplicity, we ignore the dependence of I on the frequency ν of the photons. This approximation is physically irrelevant, but this simplification allows us to concentrate on some issues of the modelling and numerical simulation, leaving aside some important but well-documented problems about frequency dependence (see for instance [19, 41, 44] and the references therein). The radiative intensity I is solution of the kinetic equation

$$\frac{1}{c}\partial_t I + \mathbf{\Omega} \cdot \nabla_{\mathbf{x}} I = \sigma_s(\langle I \rangle - I), \quad t \in \mathbb{R}, \mathbf{x} \in \mathbb{R}^3, \mathbf{\Omega} \in \mathcal{S}^2, \tag{1}$$

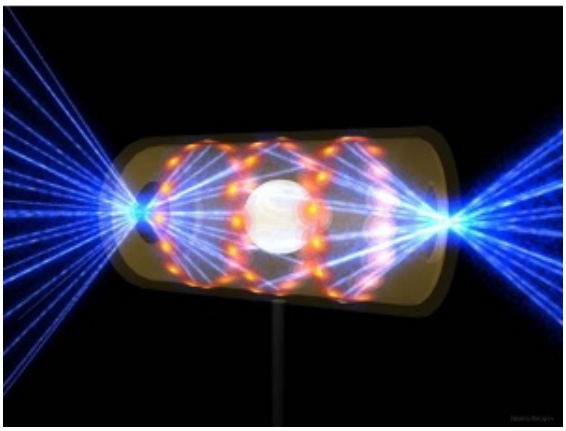

Figure 1: Inertial confinement fusion: indirect drive.

where

$$\langle I \rangle = \frac{1}{|\mathcal{S}^2|} \int_{\mathcal{S}^2} I(t, \mathbf{x}, \mathbf{\Omega}) d\mathbf{\Omega},$$

$\nabla_{\mathbf{x}}$ is the space gradient and $\sigma_s = \sigma_s(\mathbf{x}) \geqslant 0$ the scattering cross-section. This source term represents a density of photons changing direction because of collisions. Another important approximation we make here is to neglect emission-absorption terms, which read $\sigma_a(aT^4 - I)$ in the right-hand side of (1), and is of high importance in the applications we have in mind. Here again, we believe that including such a term is not difficult in what follows, but we avoid the corresponding technical difficulties. An important property of equation (1) is that its solution satisfies the maximum principle, that is,

$$\forall t > 0, \qquad \sup_{\mathbf{x} \in \mathbb{R}^3,\ \mathbf{\Omega} \in \mathcal{S}^2} I(t, \mathbf{x}, \mathbf{\Omega}) = \sup_{\mathbf{x} \in \mathbb{R}^3,\ \mathbf{\Omega} \in \mathcal{S}^2} I(0, \mathbf{x}, \mathbf{\Omega}). \tag{2}$$

Of course, such a property is valid if the equation is set in the whole space $\mathbb{R}^3$, or with appropriate boundary conditions. Property (2) is a simple application of the method of characteristics.

The kinetic equation (1) is set in a six-dimensional phase space (one for the time variable, three for the position variable, and two for the propagation direction variable). A direct discretization is therefore highly expensive. Different kind of methods have been proposed to solve this equation. A natural approach is to use a Monte Carlo approximation [31, 40]. These methods have the advantage of being essentially dimension-independent, with a rather simple implementation if one sticks to standard transport Monte Carlo schemes. However, statistical noise may be prohibitively large, since the rate of convergence is $1/\sqrt{N}$, where N is the number of particles, directly related to the computational cost. In addition, the cross sections in (1) may be very large, which implies stability issues, hence implicitation of the method is necessary [16]. Another approach is the discrete ordinate method, it consists in using a finite difference approximation for the velocity directions $\mathbf{\Omega}$ [7, 8, 36, 39]. This method suffers from so-called ray-effects [37]. In order to solve it, a large number of discretization directions (that is, of degrees of freedom) is necessary, which makes the method expensive. Another kind of discretization, considered in [34] for instance, amounts to expand I on the basis of spherical harmonics with respect to $\mathbf{\Omega}$. This method may prove fairly accurate in

case of smooth solutions. However, it suffers from violating the maximum principle satisfied by (1). Several methods have been proposed to solve this issue [23, 32]. Here again, a large number of spherical harmonics may be needed to give accurate results, which implies high numerical costs.

In this contribution, we focus on moment models [10, 30, 36, 39] which allow to decrease the phase space dimension. They consist in writing a set of equations on some means of the radiative intensity called moments. A natural way to derive such a model consists in integrating the equation against 1 and against $\mathbf{\Omega}$. Defining the radiative energy, the radiative flux and the radiative pressure by

$$\begin{cases} E(t,\mathbf{x}) = \dfrac{1}{c}\displaystyle\int_{\mathcal{S}^2} I(t,\mathbf{x},\mathbf{\Omega})d\mathbf{\Omega}, \\ \mathbf{F}(t,\mathbf{x}) = \displaystyle\int_{\mathcal{S}^2} \mathbf{\Omega} I(t,\mathbf{x},\mathbf{\Omega})d\mathbf{\Omega}, \qquad\qquad t\in\mathbb{R}, \mathbf{x}\in\mathbb{R}^3 \\ \mathbf{P}(t,\mathbf{x}) = \dfrac{1}{c}\displaystyle\int_{\mathcal{S}^2} \mathbf{\Omega}\otimes\mathbf{\Omega} I(t,\mathbf{x},\mathbf{\Omega})d\mathbf{\Omega}, \end{cases} \tag{3}$$

we obtain the system

$$\begin{cases} \partial_t E + \operatorname{div}(\mathbf{F}) = 0, \\ \dfrac{1}{c}\partial_t \mathbf{F} + c\,\operatorname{div}(\mathbf{P}) = -\sigma_s \mathbf{F}. \end{cases} \tag{4}$$

Let us note that $E(t,\mathbf{x})\in\mathbb{R}$, $\mathbf{F}(t,\mathbf{x})\in\mathbb{R}^3$ and $\mathbf{P}(t,\mathbf{x})\in\mathcal{M}_3(\mathbb{R})$, the set of real-valued 3×3 matrices. This new system is simpler than (1): we have replaced a scalar equation by a system, but the variable $\mathbf{\Omega}$ is now integrated out, and we no longer need to discretize it. However, the system is not closed for now: we have four equations for ten unkwnowns (one for E, three for $\mathbf{F}$, and six for $\mathbf{P}$, since it is a symmetric matrix). The strategy is thus to close the system by deriving an expression of $\mathbf{P}$ as a function of $E, \mathbf{F}$. The choice of this relation is crucial both from a modeling and a numerical point of view. In particular, $I\geqslant 0$ implies that the energy is nonnegative:

$$E \geqslant 0, \tag{5}$$

and that the flux is limited

$$|\mathbf{F}| \leqslant cE. \tag{6}$$

The closure should imply (5) and (6).
Another important property of (1) is the diffusion limit: if σ_s and t are large, then a good approximation is given by the diffusion equation on E [7, 8, 36, 39]

$$\partial_t E - \operatorname{div}\Big(\frac{c}{3\sigma_s}\nabla E\Big) = 0. \tag{7}$$

In the application we have in mind, this limit is of importance. Indeed, in the experimental setting, both transparent regions (σ_s small) and highly diffusive regions (σ_s large) are present, as we can see on Figure 2. Thus, the closure should preserve this diffusive regime.
Several approaches have been proposed to derive such closure relations. The simplest one consists simply in assuming that I is an affine function of $\mathbf{\Omega}$, that is, $I = \dfrac{cE}{4\pi} + \dfrac{\mathbf{F}\cdot\mathbf{\Omega}}{4\pi}$, which gives $\mathbf{P} = \dfrac{E}{3}\mathbf{Id}$. This model, usually called P_1, is equivalent to the decomposition on spherical harmonics mentioned

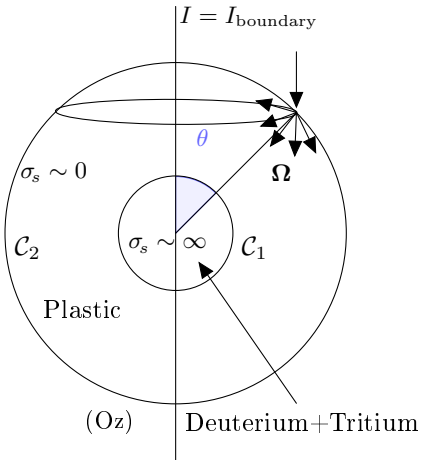

Figure 2: Idealized configuration of an ICF target.

above, provided only first and second order terms of the development are considered. This model satisfies the diffusion limit, but is rather crude in the transport regime, and does not satisfy (5) nor (6) except in one dimension (slab geometry). A maximum entropy principle has been used in [10] for deriving the so-called M_1 model in which an explicit closure is obtained. An advantage of this approach is to recover properties (5)-(6) while preserving the diffusion limit. In spite of these theoretical assets, we do not consider this model here for a reason we explain later.

The starting point of our contribution is a linear model named P_1' and introduced in [42] for a radially symmetric geometry. This model, recalled in Section 1 and written in spherical coordinates, is not proved to ensure the positivity of the energy and the limitation of the flux yet. However it satisfies the diffusion limit (Section 1) and its behavior in the case of a radially symmetric target implosion is more accurate than the M_1 model. This fact is illustrated on Figure 3. On the left hand side, we have plotted the velocity of the interface between the plastic of the target and the hydrogen gas. The black curve corresponds to a Monte Carlo simulation, which is considered as a reference. The blue curve corresponds to the use of P_1' model. Red and green curves correspond to the diffusion approximation, and to the M_1 model, respectively. The right plot represents the Eddington factor P_{RR}/E as a function of the spherical radius R (distance to the center of the target) at time $t = 1.5 \times 10^{-8} s$. The green curve is associated with the M_1 model, the blue one with the P_1' model and the black one is the Monte Carlo solution. On both plots, one can see that the P_1' model is much more adapted to this case. As for the Monte Carlo calculation, it provides an Eddington factor smaller than $1/3$ unlike the M_1 model. More explanations of this better behavior are given in Section 1.3 below.

The aim of this article is to propose an extension of the P_1' model to a cylindrical geometry. To do so, we focus on the target rather than considering the complete geometry of the cylinder. The cylindrical symmetry is represented by an axisymmetric condition at the boundary of the simulation (Figure 2). These geometrical considerations are the starting point of all our models.

Several models are proposed, that satisfy the diffusion limit. Of course, numerical schemes used to discretize these models should satisfy the diffusion limit at the discrete level. Such schemes are

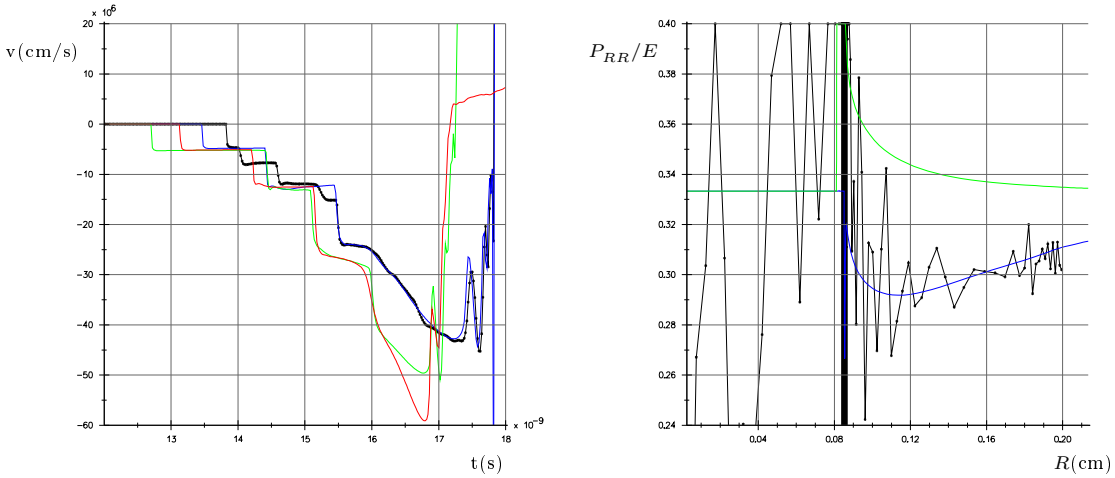

Figure 3: **Left:** plot of the velocity of the interface between the solid layer of the target and the (inner) gaseous DT as a function of time. The black curve is a Monte Carlo simulation (reference), the blue one a P_1' simulation, the green one a M_1 simulation, and the red one a diffusion approximation. **Right :** the corresponding Eddington factor as a function of R at time $1.5 \times 10^{-8} s$, that is, just before focus.

called asymptotic preserving (AP). Numerical experiments show that this is usually not the case of standard finite volume methods [5, 9, 17, 20, 27]. Specific corrections are needed in order to have a correct behavior in diffusion regimes. In this paper, we have studied this aspect in one dimension only, since it is already a challenge. Extension to higher dimension is possible but not straightforward [17]. An alternative would be to use Galerkin discontinuous methods [28], which are AP, at least for second-order (i.e. piecewise affine) discretization.

The article is organized as follows: in Section 1, we review some important properties of the 1D radial P_1' model. In particular, we recall that in the pure transport case ($\sigma_s = 0$), it gives a solution which coincides with that of (1). Actually, we also prove that such a property cannot hold if spherical symmetry assumption is dropped. This is why, in Section 2, we propose a way to extend this model to axisymmetric geometries. Finally, Section 3 proposes some numerical experiments. They are restricted to the radially symmetric case, but we plan to consider higher dimension in the near future. In this one-dimensional setting, we use the ideas of [9] to build an AP scheme, and study its consistency and stability, before giving some numerical results.

Before proceeding, we fix the notations we will use throughout the paper:

Notation. *The spherical frame* $(\mathbf{e}_R, \mathbf{e}_\theta, \mathbf{e}_\varphi)$ *is represented on Figure 4. Note that the spherical radius vector is denoted by* R *whereas the cylindrical one is denoted by* r.
In the mobile frame $(\mathbf{e}_R, \mathbf{e}_\theta, \mathbf{e}_\varphi)$*, the direction of the photons* $\mathbf{\Omega}$ *is also expressed in spherical coordinates. Space angles are denoted by greek lowercase letters* θ, ϕ*. On the contrary, the velocity spherical angles are denoted by greek capital letters* Θ, Φ.

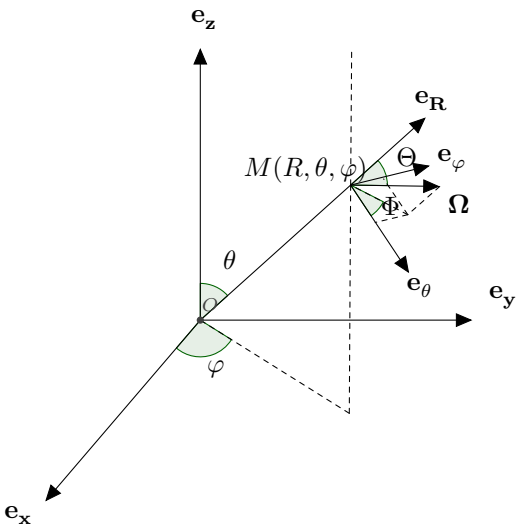

Figure 4: Representation of spherical coordinates.

1 Theoretical study of a radial model: P_1'

In this Section, we recall the derivation of the model referenced as P_1' in [42]. This model involves the first three moments E, $\mathbf{F}$ and $\mathbf{P}$, defined by (3), and solutions of equations (4). In the spherical frame (Figure 4), we denote the flux and pressure components by

$$\mathbf{F} = (F_R, F_\theta, F_\varphi), \quad \mathbf{P} = \begin{pmatrix} P_{RR} & P_{R\theta} & P_{R\varphi} \\ P_{R\theta} & P_{\theta\theta} & P_{\theta\varphi} \\ P_{R\varphi} & P_{\theta\varphi} & P_{\varphi\varphi} \end{pmatrix}.$$

The P_1' model closes the system (4) with geometric considerations in the radially symmetric case.

1.1 Derivation of the P_1' model

The intensity is assumed to be radially symmetric as in Section 1.2. Thus I is a function of t, R and $\mu = \mathbf{\Omega} \cdot \mathbf{e}_R = \cos(\Theta)$, the projection of the direction of photons $\mathbf{\Omega}$ on the vector $\mathbf{e}_R$ (Figure 4). We first write Equations (4) in spherical coordinates. The moments are evaluated in the basis $(\mathbf{e}_R, \mathbf{e}_\theta, \mathbf{e}_\varphi)$ using

$$\mathbf{\Omega} = \Big(\mu, \sqrt{1-\mu^2}\cos(\Phi), \sqrt{1-\mu^2}\sin(\Phi)\Big), \quad \mu \in [-1,1], \Phi \in [0, 2\pi]. \tag{8}$$

The energy and the flux reduce to

$$E = \frac{2\pi}{c}\int_{-1}^{1} I(t,R,\mu)d\mu, \quad F_R = 2\pi\int_{-1}^{1} \mu I(t,R,\mu)d\mu, \quad F_\theta = F_\varphi = 0.$$

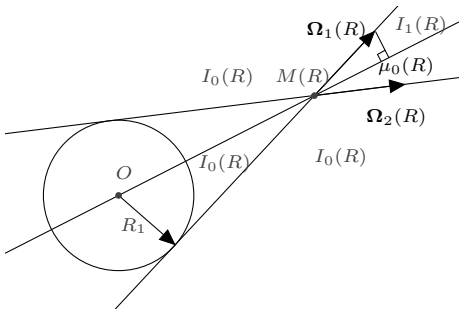

Figure 5: In the case of vacuum ($\sigma_s = 0$): $I(t, R, \mathbf{\Omega}) = I_0(t, R)$ if $\mathbf{\Omega} \cdot \mathbf{e}_R < \mu_0(R)$ and $I(t, R, \mathbf{\Omega}) = I_1(t, R)$ if $\mathbf{\Omega} \cdot \mathbf{e}_R > \mu_0(R)$ (the shadow cone of the target).

Furthermore, the pressure tensor is diagonal and its three coefficients are linked by

$$P_{\theta\theta} = \frac{1}{2}(E - P_{RR}) = P_{\varphi\varphi}. \tag{9}$$

Using radial symmetry, the divergence of the flux reads

$$\mathrm{div}(\mathbf{F}) = \frac{1}{R^2}\partial_R(R^2 F_R),$$

and the first component of the divergence of the pressure is given by

$$\mathrm{div}(\mathbf{P})_R = \partial_R(P_{RR}) + \frac{2P_{RR} - P_{\theta\theta} - P_{\varphi\varphi}}{R}.$$

Using (4), the general one dimensional radial equations satisfied by E, F_R are thus

$$\begin{cases} \partial_t E + \dfrac{1}{R^2}\partial_R(R^2 F_R) = 0, \\ \dfrac{1}{c}\partial_t F_R + c\partial_R(P_{RR}) + c\dfrac{3P_{RR} - E}{R} = -\sigma_s F_R. \end{cases}$$

We are going to close the system i.e. to express the pressure P_{RR} as a function of E and F_R.
Let us first note that choosing $P_{RR} = E/3$ gives the so-called P_1 model [8]. Leaving aside this choice, we use the geometry of the experiment (Figure 5) to derive a closure which is more adapted to this setting.
If $\sigma_s = 0$, the method of characteristics implies that the solution to (1) is of the following form:

$$I(t, R, \mu) = I_0(t, R)\mathbb{1}_{-1 \leqslant \mu \leqslant \mu_0(R)} + I_1(t, R)\mathbb{1}_{\mu_0(R) \leqslant \mu \leqslant 1}, \tag{10}$$

where $\mu_0(R) = \mathbf{\Omega}_0(R) \cdot \mathbf{e}_R$ delimits the boundary of the shadow cone of the target (see Figure 5). Assuming this structural assumption on the intensity, one can evaluate the energy and the flux

$$E = \frac{2\pi}{c}\Big(I_1(t, R)(1 - \mu_0(R)) + I_0(t, R)(1 + \mu_0(R))\Big),$$

$$F_R = \pi \Big(1 - \mu_0^2(R)\Big) \Big(I_1(t,R) - I_0(t,R)\Big).$$

The inversion of this linear system leads to

$$I_0(t,R) = \frac{cE}{4\pi} - \frac{F_R}{2\pi(1+\mu_0(R))}, \quad I_1(t,R) = \frac{cE}{4\pi} + \frac{F_R}{2\pi(1-\mu_0(R))}.$$

Thus the pressure P_{RR} satisfies

$$P_{RR} = \frac{2\pi}{c}\Big(I_1(t,R)\frac{1-\mu_0^3(R)}{3} + I_0(t,R)\frac{1+\mu_0^3(R)}{3}\Big) = \frac{E}{3} + \frac{2\mu_0(R)F_R}{3c}. \tag{11}$$

Using this closure relation, we define the P_1' model as

$$\begin{cases} \partial_t E + \dfrac{1}{R^2}\partial_R(R^2 F_R) = 0, \\ \dfrac{1}{c}\partial_t F_R + \dfrac{c}{3}\partial_R E + \dfrac{2}{3}\partial_R(\mu_0(R)F_R) + \dfrac{2}{R}\mu_0(R)F_R = -\sigma_s F_R. \end{cases} \tag{12}$$

Finally, we need to compute μ_0. In the situation represented in Figure 2, its definition is relatively clear and corresponds to the shadow cone of the target (Figure 5):

$$\mu_0(R) = \sqrt{1 - \frac{R_1^2}{R^2}}. \tag{13}$$

In more realistic situation, we do not have a clear separation between the transparent zone $R > R_1$ and the target. Hence, the definition of μ_0 needs to be adapted. In the radially symmetric case, a strategy has been proposed in [42]. It amounts to considering the equation on the second order moment $\mathbf{P}$ of Equation (1). This equation relates this second order moment to the third order one

$$\mathbf{Q}(t,\mathbf{x}) = \int_{\mathcal{S}^2} \mathbf{\Omega}\otimes\mathbf{\Omega}\otimes\mathbf{\Omega}\; I(t,\mathbf{x},\mathbf{\Omega})d\mathbf{\Omega}. \tag{14}$$

Each of them is then expressed in terms of $\mu_0(R), E, F_R$ using the structural assumption (10). Thus, one ends up with an ordinary differential equation on μ_0 which reads

$$\frac{d\mu_0}{dR} = \frac{1-\mu_0^2}{R\mu_0} - \frac{2}{3}\sigma_s. \tag{15}$$

This equation may be solved numerically. If $\sigma_s = 0$, one recovers (13). Note that obtaining an ordinary differential equation is conditioned by the radially symmetric assumption. Indeed, this symmetry leads to simplifications which do not occur in a more complicated geometry (see [42] for the details).

To treat the diffusion regime ($c \to \infty$, $\sigma_s \to \infty$), we need to rescale the P_1' model. So we introduce the scaling

$$c = \frac{\widetilde{c}}{\epsilon}, \quad \sigma_s = \frac{\widetilde{\sigma_s}}{\epsilon}. \tag{16}$$

We can then write the P_1' model as

$$\begin{cases} \partial_t E + \dfrac{1}{R^2}\partial_R(R^2 F_R) = 0, \\ \dfrac{\epsilon}{\widetilde{c}}\partial_t F_R + \dfrac{\widetilde{c}}{3\epsilon}\partial_R E + \dfrac{2}{3}\partial_R(\mu_0(R)F_R) + \dfrac{2}{R}\mu_0(R)F_R = -\dfrac{\widetilde{\sigma_s}}{\epsilon}F_R. \end{cases} \tag{17}$$

Although the limit diffusion $\epsilon \to 0$ is independent of μ_0, it is interesting to study the behaviour of μ_0 in this limit. Indeed, (15) becomes

$$\frac{d\mu_0}{dR} = \frac{1-\mu_0^2}{R\mu_0} - \frac{2}{3}\frac{\widetilde{\sigma_s}}{\epsilon}.$$

Hence, a formal expansion of μ_0 in powers of ϵ gives

$$\mu_0(R) = \frac{3}{2R\widetilde{\sigma_s}(R)}\epsilon + \frac{27\widetilde{\sigma_s}'(R)}{8\widetilde{\sigma_s}(R)^4 R^2}\epsilon^3 + O\left(\epsilon^5\right). \tag{18}$$

Actually, if σ_s is constant, one easily proves that we have the exact formula $\mu_0(R) = \dfrac{3}{2R\widetilde{\sigma_s}}\epsilon$. In any case, μ_0 vanishes in the limit $\epsilon \to 0$. Hence, it is expected that all the properties of the model in this limit be consistent with those of the P_1 model.

In the following, we keep c and σ_s instead of $\widetilde{c}$ and $\widetilde{\sigma_s}$ for the sake of clarity. We show in the next Section that the system formally tends to the diffusion equation (7) as ϵ goes to 0.

1.2 Theoretical properties of the model

This Section deals with some properties of the P_1' model, which now reads

$$\begin{cases} \partial_t E + \dfrac{1}{R^2}\partial_R(R^2 F_R) = 0, \\ \dfrac{\epsilon}{c}\partial_t F_R + \dfrac{c}{3\epsilon}\partial_R E + \dfrac{2}{3}\partial_R(\mu_0(R)F_R) + \dfrac{2}{R}\mu_0(R)F_R = -\dfrac{\sigma_s}{\epsilon}F_R. \end{cases} \tag{19}$$

We first prove an energy equality, then study the diffusion limit of the model. Unless otherwise stated, we assume that μ_0 is nonnegative and nondecreasing with respect to R, which is physically relevant. We also prove that the P_1' model formally tends to the diffusion equation (7) as ϵ goes to 0.

The P_1' model (19) reads as the following linear system:

$$\partial_t \mathbf{U} + \frac{1}{R^2\epsilon}\partial_R(R^2\mathbf{A}(R)\mathbf{U}) = \frac{1}{\epsilon}\mathbf{G}_\epsilon(R)\mathbf{U}, \tag{20}$$

where

$$\mathbf{U} = \begin{pmatrix} \frac{c}{\epsilon\sqrt{3}}E \\ F_R \end{pmatrix}, \quad \mathbf{A}(R) = \begin{pmatrix} 0 & \frac{c}{\sqrt{3}} \\ \frac{c}{\sqrt{3}} & \frac{2c\mu_0(R)}{3} \end{pmatrix}, \quad \mathbf{G}_\epsilon(R) = \begin{pmatrix} 0 & 0 \\ \frac{2c}{\sqrt{3}R} & -\frac{2c\mu_0(R)}{3R} - \frac{c\sigma_s(R)}{\epsilon} \end{pmatrix}. \tag{21}$$

The matrix $\mathbf{A}$ is symmetric, and

$$\mathbf{G}_\epsilon + {}^t\mathbf{G}_\epsilon - \frac{1}{R^2}\partial_R\left(R^2\mathbf{A}\right) = \begin{pmatrix} 0 & 0 \\ 0 & -\frac{8c\mu_0(R)}{3R} - \frac{2c\sigma_s(R)}{\epsilon} - \frac{2c\mu_0'(R)}{3} \end{pmatrix}, \tag{22}$$

is nonpositive, provided μ_0 is nonnegative and nondecreasing. Hence, (20) is a so-called Friedrichs system with a linear relaxation term [13, 12, 14, 15, 18]. As a consequence, it is hyperbolic. In our case, the P_1' model is strictly hyperbolic, since it has two distinct eigenvalues.
This allows to prove the following Proposition.

Proposition 1.1 (Energy equality)**.** *Assume that $\mu_0 \geqslant 0$ is a nondecreasing function of R. If $\mathbf{U} \in W^{1,1}$ is a solution of the symmetrized P_1' model* (20) *then*

$$\partial_t (\mathbf{U} \cdot \mathbf{U}) + \frac{1}{R^2 \epsilon} \partial_R (R^2 \mathbf{U} \cdot \mathbf{A}\mathbf{U}) = \frac{1}{\epsilon} \mathbf{Q}_\epsilon(\mathbf{U}), \tag{23}$$

where the quadratic form

$$\mathbf{Q}_\epsilon(\mathbf{U}) = \mathbf{U} \cdot \Big(\mathbf{G}_\epsilon + {}^t\mathbf{G}_\epsilon - \frac{\partial_R(R^2 \mathbf{A})}{R^2} \Big) \mathbf{U},$$

is nonpositive and $\cdot$ is the canonical scalar product of $\mathbb{R}^2$.

Proof. The identity (23) immediately results from (20). The matrix defining the quadratic form $\mathbf{Q}_\epsilon$ is given by (22). As we already pointed out above, its eigenvalues are nonpositive for all R because μ_0 is a nonnegative nondecreasing function of R and σ_s is nonnegative. □

An important question when dealing with hyperbolic systems is the determination of the eigenvalues and eigenvectors of the corresponding matrix. Here, the eigenvalues of A are given by

$$\lambda^\pm(R) = \frac{c}{3} \left(\mu_0(R) \pm \sqrt{\mu_0(R)^2 + 3} \right). \tag{24}$$

We always have $\lambda^+(R) > 0$ and $\lambda^-(R) < 0$ and the corresponding right eigenvectors are

$$\mathcal{R}^\pm(R) = \begin{pmatrix} \sqrt{3} \\ \frac{3}{c} \lambda^\pm(R) \end{pmatrix}.$$

Hence, the Riemann invariants of (20) read

$$w^\pm(R) = cE + \epsilon \frac{3}{c} \lambda^\mp(R) F_R. \tag{25}$$

Remark 1.2. *In the special case $\mu_0 \equiv 0$, we recover the classical P_1 model, with the corresponding eigenvalues $\pm \dfrac{c}{\sqrt{3}}$ and the Riemann invariants $cE \mp \epsilon \sqrt{3} F_R$.*

Let us give a rapid analysis of the diffusion limit.

Proposition 1.3 (Diffusion limit)**.** *Assume the following expansions on E and F_R,*

$$\begin{cases} E = E^{(0)} + \epsilon E^{(1)} + \mathcal{O}(\epsilon^2), \\ F_R = F_R^{(0)} + \epsilon F_R^{(1)} + \mathcal{O}(\epsilon^2), \end{cases} \tag{26}$$

as ϵ goes to 0 where (E, F_R) is a solution to (19)*. Then $E^{(0)}$ is a solution to*

$$\partial_t E^{(0)} - \operatorname{div} \Big(\frac{c}{3\sigma_s} \nabla E^{(0)} \Big) = 0. \tag{27}$$

Proof. We only give a formal proof of this result. A rigourous one can be found for instance in [17, Theorem 4.3]. After replacing the expansions (26) in (19), we identify the terms of same order in ϵ. The term corresponding to ϵ^{-1} of the equation over F_R leads to

$$F_R^{(0)} = -\frac{c}{3\sigma_s(R)}\partial_R E^0. \tag{28}$$

Then, the term corresponding to ϵ^0 of the equation on E yields

$$\partial_t E^{(0)} + \frac{1}{R^2}\partial_R(R^2 F_R^{(0)}) = 0. \tag{29}$$

We get the diffusion equation (27) by inserting (28) into (29). □

To close this Section, we mention that we have not been able to prove or disprove the positivity of the energy and the limitation of the flux (6). However, in the case $\mu_0 = 0$, we recover the usual P_1 model, which does not satisfy the maximum principle [33].

Let us also mention that the free streaming regime is not reproduced by the present model. Indeed, such regime corresponds to a closure in which the Eddington factor $\gamma = P_{RR}/E$ satisfies the following property :

$$\gamma(f) \underset{f\to 1}{\longrightarrow} 1, \tag{30}$$

where $f = F_R/(cE)$. Here, we have

$$\gamma(f) = \frac{1}{3} + \frac{2}{3}\mu_0 f,$$

which clearly does not satisfy (30).
Let us note that the present model allows situations in which $\gamma < 1/3$, which is not the case of most moment models [29], as for instance M_1 model (see Figure 3).

1.3 Stationary solutions in pure transport

In this Section, we compute the stationary solutions of the radiative transfer equation (1) and of the P_1' model (19) in the pure transport case ($\sigma_s = 0$) for an axisymmetric boundary condition. These computations have three purposes. First, it shows that the P_1' model preserves the stationary solutions of (1) when $\sigma_s = 0$ for a radially symmetric boundary condition. Second, it proves that the stationary P_1' model is ill-posed for a nonradial boundary condition. Third, it allows to derive some moment models, well-posed for an nonradial boundary condition, which are generalizations of the P_1' model. The idea is to take into account the exact solution of the radiative transfer equation in the case $\sigma_s = 0$ in the structural assumption as we did for P_1' model in the radially symmetric case.

1.3.1 Solutions of the radiative transfer equation

In this paragraph, we compute the stationary solutions of the radiative transfer equation when $\sigma_s = 0$ for an axisymmetric boundary condition. We consider two spheres of radius $0 < R_1 < R_2$ (Figure 6). In the domain

$$\mathcal{D} = \left\{\mathbf{x} \in \mathbb{R}^3, \quad R_1 < |x| < R_2\right\},$$

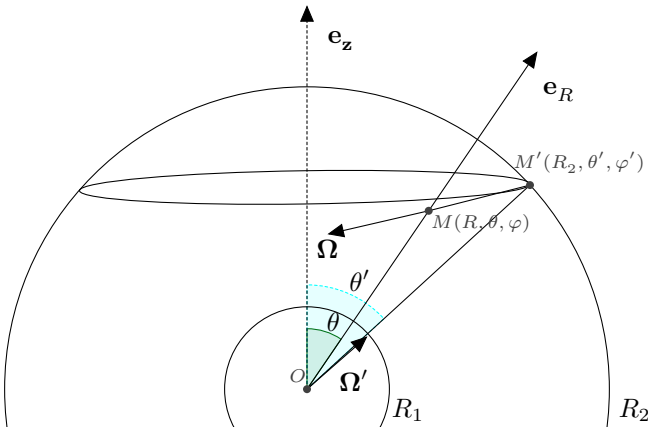

Figure 6: Definition of θ' and M'.

the radiative intensity is supposed to satisfy the transport equation

$$\frac{1}{c}\partial_t I + \mathbf{\Omega} \cdot \nabla_{\mathbf{x}} I = 0, \quad t \in \mathbb{R}, \mathbf{x} \in \mathcal{D}, \mathbf{\Omega} \in \mathcal{S}^2. \tag{31}$$

An axisymmetric boundary condition on the radiative intensity is prescribed at R_2: this intensity is an expansion on the Legendre polynomial basis [1, 38, 43] given by

$$I_{R_2}(t, \theta, \varphi, \mathbf{\Omega}) = \sum_l I_l(t) P_l(\cos(\theta)), \quad \text{if } \mathbf{\Omega} \cdot \mathbf{e}_R < 0, \tag{32}$$

where P_l is the l^{th} Legendre polynomial. Note that this intensity is chosen independent of $\mathbf{\Omega}$. We impose zero incoming flux at R_1:

$$I_{R_1}(t, \theta, \varphi, \mathbf{\Omega}) = 0, \quad \text{if } \mathbf{\Omega} \cdot \mathbf{e}_R > 0.$$

Our purpose is to compute the first moments of the intensity at an arbitrary space position R belonging to (R_1, R_2). The following computation is a generalization of [22], in which only $I(R_1)$ is computed.
The intensity is constant along the characteristics of Equation (1). The intensity at the point $M(R, \theta, \varphi)$ in the direction $\mathbf{\Omega}$ originates from the point $M'(R_2, \theta', \varphi')$ (Figure 6). Thus it is given by

$$I(t, \mathbf{x}, \mathbf{\Omega}) = I_{R_2}\left(t - \frac{MM'}{c}, \theta', \varphi'\right) = \mathbb{1}_{\{\mathbf{\Omega} \cdot \mathbf{e}_R < \mu_0(R)\}} \sum_l I_l\left(t - \frac{MM'}{c}\right) P_l(\cos(\theta'(\mathbf{\Omega}))), \tag{33}$$

where μ_0 is defined by (13) and represents the limit of the shadow cone (Figure 5). Using (8), a moment $\mathfrak{m}$ associated with the polynomial $P \in \mathbb{R}[X_1, X_2, X_3]$ (the space of three variables polynomials) writes

$$\mathfrak{m} = \frac{1}{c} \int_{-1}^{\mu_0} \int_0^{2\pi} P(\mu, \sqrt{1-\mu^2}\cos(\Phi), \sqrt{1-\mu^2}\sin(\Phi)) I(t, \mathbf{x}, \mu, \Phi) d\mu d\Phi. \tag{34}$$

In the case of a stationary radial boundary condition

$$I_{R_2}(t,\theta,\varphi,\mathbf{\Omega}) = I_{R_2}, \tag{35}$$

the computation immediately leads to

$$E = \frac{2\pi}{c}\Big(1+\frac{\sqrt{R^2-R_1^2}}{R}\Big)I_{R_2}, \quad F_R = -\frac{\pi R_1^2}{R^2}I_{R_2}. \tag{36}$$

For a boundary condition which is not radially symmetric, we have to express $\cos(\theta'(\mathbf{\Omega}))$ in terms of μ and Φ. This is achieved using the addition theorem on Legendre polynomials [11]

$$P_l(\cos(\theta'(\mathbf{\Omega}))) = \sum_{m=-l}^{l}(-1)^m P_l^{-m}(\cos(\theta))P_l^m(\mu')e^{im\Phi}, \quad l\in\mathbb{N}$$

where $\mu' = \mathbf{\Omega}'\cdot\mathbf{e}_R$ (note that $\mu'\neq\cos\theta'$) and

$$P_l^m(x) = (-1)^m(1-x^2)^{\frac{m}{2}}\frac{\partial^m}{\partial x^m}P_l(x), \quad l,m\in\mathbb{N}, |m|\leqslant l.$$

Thus (33) now reads

$$I(t,\mathbf{x},\mathbf{\Omega}) = I(\mathbf{x},\mathbf{\Omega}) = \mathbb{1}_{\{\mathbf{\Omega}\cdot\mathbf{e}_R<\mu_0(R)\}}\sum_l I_l(t)\sum_{m=-l}^{l}(-1)^m P_l^{-m}(\cos(\theta))P_l^m(\mu')e^{im\Phi}. \tag{37}$$

Note that the addition theorem allows to express the boundary condition in the plane $(O,\mathbf{\Omega},\mathbf{e}_R)$. We can relate the projections μ' and μ. The Al Qashi theorem (Figure 7) yields

$$\mu' = \frac{R_2^2+R^2-MM'^2}{2RR_2}, \quad \mu = \frac{R^2+MM'^2-R_2^2}{2RMM'}, \quad MM' = \sqrt{R_2^2+R^2-2RR_2\mu'}.$$

Moreover, μ' and μ satisfy the relation

$$\mu = \frac{R-\mu' R_2}{MM'} = \frac{R-\mu' R_2}{\sqrt{R_2^2+R^2-2RR_2\mu'}}. \tag{38}$$

We now evaluate the moments. The variable change (38) is applied to (34) to get

$$\mathfrak{m} = \frac{1}{c}\int_{\mu_{\min}}^{1}\int_0^{2\pi}\overline{P}(\mu',\Phi)I(t,\mathbf{x},\mu',\Phi)\frac{R_2^2(R_2-R\mu')}{MM'^3}d\mu' d\Phi,$$

where

$$\mu_{\min} = \tfrac{R_1^2}{R_2R} + \tfrac{\sqrt{(R_2^2-R_1^2)(R^2-R_1^2)}}{R_2R},$$

and

$$\overline{P}(\mu',\Phi) = P\left(\tfrac{R-\mu' R_2}{MM'}, \sqrt{1-\left(\tfrac{R-\mu' R_2}{MM'}\right)^2}\cos(\Phi), \sqrt{1-\left(\tfrac{R-\mu' R_2}{MM'}\right)^2}\sin(\Phi)\right).$$

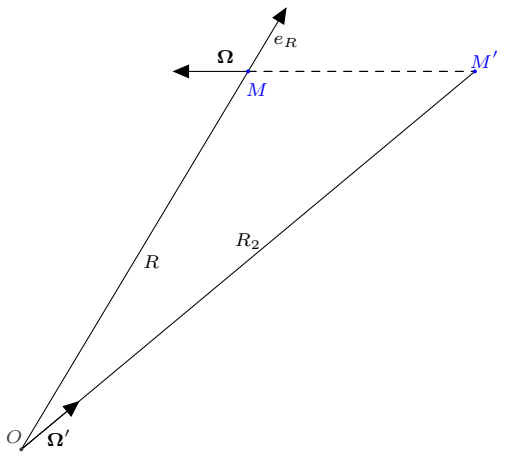

Figure 7: Points M and M'.

To simplify the expression of the integrand, we use a second change of variable:

$$\mu_n = \tfrac{MM'^2}{R_2^2} = 1 + \nu^2 - 2\nu\mu',$$

where $\nu = R/R_2$. Consequently,

$$\mathfrak{m} = \frac{1}{c}\int_{(1-\nu)^2}^{\mu_n(\mu_{\min})}\int_0^{2\pi} \widetilde{P}(\mu_n,\Phi) I(t,\mathbf{x},\mu_n,\Phi)\frac{1-\nu^2+\mu_n}{4\nu\mu_n^{\frac{3}{2}}} d\mu_n d\Phi,$$

where

$$\widetilde{P}(\mu_n,\Phi) = P\left(\tfrac{\nu^2-1+\mu_n}{2\nu\sqrt{\mu_n}}, \sqrt{1-\left(\tfrac{\nu^2-1+\mu_n}{2\nu\sqrt{\mu_n}}\right)^2}\cos(\Phi), \sqrt{1-\left(\tfrac{\nu^2-1+\mu_n}{2\nu\sqrt{\mu_n}}\right)^2}\sin(\Phi)\right),$$

and

$$\mu_n\left(\mu_{\min}\right) = \left(\frac{\sqrt{R_2^2-R_1^2}-\sqrt{R^2-R_1^2}}{R_2}\right)^2.$$

These integrals can be computed for any polynomial using the intensity (37). For the sake of conciseness, we do not give the details. We rather explain how this framework can be used for building generalizations of the P_1' model to a cylindrical geometry. The idea is to reproduce the exact solution of the radiative transfer equation when $\sigma_s = 0$ for the boundary condition (32) for

$l \in \{0,1,2\}$ (P_1' preserves exactly the solution when $l=0$: see Section 1.3.2 below). The structural assumption on the intensity adapted from the P_1' model is

$$I(t,\mathbf{x},\mathbf{\Omega}) = \sum_{l=0}^{2} P_l(\cos(\theta'(\mathbf{\Omega}))) \left[I_l(t,\mathbf{x}) \mathbb{1}_{-1 \leqslant \mu \leqslant \mu_0(R)}(\mathbf{\Omega}) + J_l(t,\mathbf{x}) \mathbb{1}_{\mu_0(R) \leqslant \mu \leqslant 1}(\mathbf{\Omega}) \right], \tag{39}$$

where I_l, J_l, for $l \in \{0,1,2\}$, are six unknown intensities. Then the model is composed of equations on $E, \mathbf{F}, \mathbf{P}$ and the closure involves the third order moment $\mathbf{Q}$ (14). More details are given in Section 2.2.2.

1.3.2 Stationary solutions of the P_1' model

The purpose of this Section is to compute the stationary solutions of the P_1' model for axisymmetric boundary conditions in pure transport ($\sigma_s = 0$). This is useful for several reasons. First, it justifies the better accuracy of the P_1' model compared to P_1 and M_1 for the isotropic target implosion (Figure 3). Indeed, we show that for a radially symmetric boundary condition, the P_1' model has the same stationary solutions as the radiative transfer equation in pure transport (36). Thus, the good accuracy in the transparent part of the target implies a precise evaluation of the flux at the boundary of the highly diffusive zone. Second, it shows the ill-posedness of the P_1' model for nonradial boundary conditions: the P_1' model thus needs to be generalized to non radially symmetric configurations. Third, exact solutions are useful for further evaluation of the models and of the numerical schemes implemented.
The starting point is the stationary P_1' model in pure transport, in spherical coordinates, for an axisymmetric configuration $E = E(R,\theta)$, $\mathbf{F} = \mathbf{F}(R,\theta)$. So, let us consider the stationary system (4) written in spherical coordinates:

$$\begin{cases} \dfrac{1}{R^2}\partial_R(R^2 F_R) + \dfrac{1}{R\sin(\theta)}\partial_\theta(\sin(\theta)F_\theta) = 0, \\ \dfrac{c}{3}\partial_R E + \partial_R\left(\dfrac{2\mu_0(R)F_R}{3}\right) + \dfrac{2\mu_0(R)F_R}{R} = 0, \\ \dfrac{c}{3R}\partial_\theta E - \dfrac{\mu_0(R)}{3R}\partial_\theta F_R = 0. \end{cases} \tag{40}$$

where the pressure tensor is defined by the relations (9) and (11).

Proposition 1.4. *Assume that $0 < R_1 < R_2$, and that $\mu_0 \geqslant 0$ satisfies $\mu_0(R_1) = 0$. Let $E, \mathbf{F} \in L^2\left[(R_1,R_2)\times(-\pi/2,\pi/2)\right]$ be a stationary solution to the P_1' system (40) with $\sigma_s = 0$. Then E, F_R are radially symmetric. Moreover E, F_R are also defined by (3), where I is a stationary solution of (31).*

Remark 1.5. *A consequence of this Proposition is that the stationary P_1' problem is ill-posed when the boundary condition is not radially symmetric.*

Remark 1.6. *Note that Proposition 1.4 states that the P_1' model is exact in the case of radially symmetric geometries, if $\sigma_s = 0$. However, this is not the case when radially symmetry is dropped, as we will see below.*

Proof. For almost all R, $E(R,\cdot), \mathbf{F}(R,\cdot) \in L^2\left[(-\pi/2,\pi/2)\right]$ can be decomposed using the hilbertian basis of Legendre polynomials P_l of $L^2\left[(-1,1)\right]$ so that

$$E(R,\theta) = \sum_i E_i(R) P_i(\cos(\theta)), \quad \mathbf{F}(R,\theta) = \sum_i \mathbf{F}_i(R) P_i(\cos(\theta)),$$

for $E_i, \mathbf{F}_i = (F_{R,i}, F_{\theta,i}, F_{\varphi,i})$ radial functions of $L^2\left[(R_1,R_2)\right], i \in \mathbb{N}$. We insert these expansions in the model (40). The third Equation of (40) gives

$$\mu_0(R) F_{R,i}(R) = c E_i(R) \quad i \neq 0, \quad \mu_0(R) F_{R,0}(R) = c(E_0(R) + f(R)), \tag{41}$$

for some function $f = f(R)$. We now use these identities in the second Equation of (40). It follows that

$$\partial_R E_0(R) + \frac{2}{R} E_0(R) + \frac{2}{3}\partial_R f(R) + \frac{2f(R)}{R} + \sum_{i\neq 0} (\partial_R E_i(R) + \frac{2}{R} E_i(R)) P_i(\cos(\theta)) = 0.$$

The uniqueness of this development yields

$$\begin{cases} E_i(R) = \dfrac{K_i}{R^2}, \quad i \neq 0, \quad K_i \in \mathbb{R} \\ \partial_R E_0(R) + \dfrac{2}{R} E_0(R) + \dfrac{2}{3}\partial_R f(R) + \dfrac{2f(R)}{R} = 0, \end{cases} \tag{42}$$

Knowing that $\mu_0(R_1) = 0$, (41) combined with the first relation of (42) implies that $\forall i \neq 0$, $\forall R$, $K_i = 0$ and $\mu_0(R) F_{R,i}(R) = c E_i(R) = 0$. Hence the energy and the radial component of the flux are radially symmetric and satisfy

$$E = E_0(R), \quad F_R = F_{R,0}(R).$$

In order to compute F_θ, we use the first Equation of (40) and find

$$F_\theta(R,\theta) = \frac{g(R)}{\sin(\theta)} + \frac{\cos(\theta)}{R\sin(\theta)} \partial_R (R^2 F_{R,0}(R)),$$

with g a function of R. The assumption $F_\theta \in L^2\left[(R_1,R_2)\times(-\pi/2,\pi/2)\right]$ leads to

$$g(R) = 0, \quad F_{R,0}(R) = \frac{K_2}{R^2}, \quad K_2 \in \mathbb{R}, \quad F_\theta = 0. \tag{43}$$

We now combine (41), the second Equation of (42) and (43) to get

$$f(R) = K_3 + \frac{3K_2\mu_0(R)}{cR^2} + \frac{6K_2}{c}\int_{R_1}^R \frac{\mu_0(s)}{s^3} ds,$$

so that

$$E(R) = -K_3 - \frac{2K_2\mu_0(R)}{cR^2} - \frac{6K_2}{c}\int_{R_1}^R \frac{\mu_0(s)}{s^3} ds.$$

Thus, we have proved that any square integrable stationary solution of the P_1' model for $\sigma_s = 0$ is radial. Let us now prove that this solution (E, F_R) satisfies (3) with I solution of (31). The condition (35) allows to compute the boundary condition on E, F_R:

$$cE(R_2) = 2\pi(1+\mu_0(R_2)) I_{R_2}, \quad F_R(R_2) = \pi(\mu_0(R_2)^2 - 1) I_{R_2}. \tag{44}$$

Using (43), (44) and (13), one gets

$$K_2 \overset{(43)+(44)}{=} \pi R_2^2(\mu_0(R_2)^2-1)I_{R_2} \overset{(13)}{=} -\pi R_1^2 I_{R_2}.$$

This gives exactly the expression of the flux in (36) obtained for the radiative transfer equation. Then the constant K_3 is given by

$$K_3 = I_{R_2}\left(\frac{2\pi\mu_0(R_2)R_1^2}{cR_2^2} - \frac{2\pi(1+\mu_0(R_2))}{c} + \frac{6\pi R_1^2}{c}\int_{R_1}^{R_2}\frac{\mu_0(s)}{s^3}ds\right),$$

and the energy

$$E = I_{R_2}\left(\frac{2\pi R_1^2\mu_0(R)}{cR^2} - \frac{2\pi R_1^2\mu_0(R_2)}{cR_2^2} + \frac{2\pi(1+\mu_0(R_2))}{c} - \frac{6\pi R_1^2}{c}\int_{R}^{R_2}\frac{\mu_0(s)}{s^3}ds\right).$$

This gives, after calculations, the value of the energy in (36). □

2 Derivation of axisymmetric models

In this Section, we present several models which are generalization of the P_1' model to cylindrical geometry. First, we simply use a change of coordinates to write P_1' in cylindrical geometry. Next, we present closures which are generalizations of P_1, and are based on the assumption that the underlying radiation intensity I is a finite combination of spherical harmonics.

We first present the structural assumption used to generalize the P_1' model. Here again, we distinguish between points being inside or outside the shadow cone of the target. The idea is to add an axisymmetric anisotropy to enrich (10) keeping the model as simple as possible. Our first choice is a kind of P_n closure [8, 36, 39]. Let us define the spherical harmonics [43]:

$$\begin{aligned} Y_l^m(\Theta,\Phi) &= \sqrt{\frac{(2l+1)(l-m)!}{4\pi(l+m)!}}P_l^m(\cos(\Theta))e^{im\Phi}, \quad && 0\leqslant m\leqslant l,\\ Y_l^{-m}(\Theta,\Phi) &= (-1)^m\overline{Y_l^m(\Theta,\Phi)}, && 0\leqslant m\leqslant l, \end{aligned}$$

with

$$P_l^m = (-1)^m(1-x^2)^{\frac{m}{2}}\frac{\partial^m P_l}{\partial x^m}, \quad l,m\in\mathbb{N}, m\leqslant l,$$

where P_l is the l^{th} Legendre polynomial. It is known that the spherical harmonics form an orthogonal basis of $L^2(\mathcal{S}^2)$ [11, 43]. The structural assumption consists in truncating the expansion on the spherical harmonics of the intensity at first order. The intensity reads

$$I(t,\mathbf{x},\mathbf{\Omega}) = \sum_{l=0,1}\sum_{m=-l}^{l} Y_l^m(\Theta,\Phi)\left[I_l^m(t,\mathbf{x})\mathbb{1}_{-1\leqslant\mu\leqslant\mu_0(R)}(\mathbf{\Omega}) + J_l^m(t,\mathbf{x})\mathbb{1}_{\mu_0(R)\leqslant\mu\leqslant 1}(\mathbf{\Omega})\right], \tag{45}$$

where $I_l^m, J_l^m \in \mathbb{R}$ are some unknown functions of time and space. Here, we point out two facts. First, the P_1' model corresponds to (45) truncated at order zero. Second, no assumption of cylindrical symmetry is made for this closure. It leads to a three dimensional model which can then be particularized to the cylindrical symmetry.

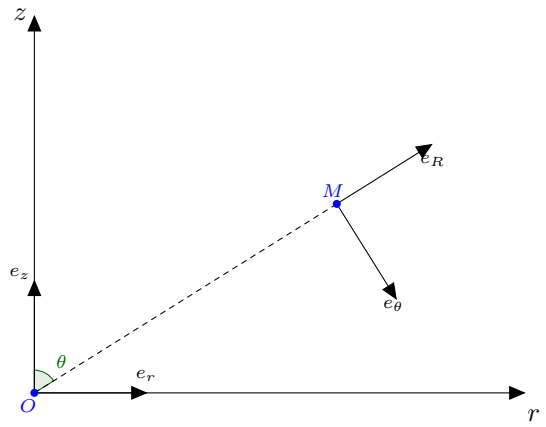

Figure 8: The basis (e_θ, e_R) in the plane (e_r, e_z).

Next, we present a strategy which takes into account the cylindrical symmetry. For this purpose, we use the structure of the exact solution of the radiative transfer in pure transport ($\sigma_s = 0$). This solution is explicit by the method of characteristics; it is characterized by the angle $\theta'(\mathbf{\Omega})$ represented on Figure 6. We replace the spherical harmonics $Y_l^m(\Theta, \Phi)$ in (45) by $P_l(\cos(\theta'))$, $l \in \mathbb{N}$. Thus the intensity is given by (39), that is,

$$I(t, \mathbf{x}, \mathbf{\Omega}) = \sum_{l=0}^{2} P_l\left(\cos(\theta'(\mathbf{\Omega}))\right) \left[I_l(t, \mathbf{x}) \mathbb{1}_{-1 \leqslant \mu \leqslant \mu_0(R)}(\mathbf{\Omega}) + J_l(t, \mathbf{x}) \mathbb{1}_{\mu_0(R) \leqslant \mu \leqslant 1}(\mathbf{\Omega}) \right],$$

where I_l, J_l, for $l \in \{0, 1, 2\}$, are six unknown intensities. More details are given in Section 2.2.2 below.
In both cases, we could have gone further in the expansion. However, we want to build nonradial models with as few equations as possible. A higher order model implies larger set of equations in the final system.

2.1 The P_1' model in cylindrical coordinates

In this Subsection, we define the P_1' model in cylindrical coordinates. It will be used as a comparison basis to test our new models. The cylindrical basis is denoted by $(\mathbf{e_r}, \mathbf{e}_\varphi, \mathbf{e_z})$. The transition from the spherical basis $(\mathbf{e}_R, \mathbf{e}_\theta, \mathbf{e}_\varphi)$ to the cylindrical one (Figure 8) is given by the matrix

$$\mathbf{R}_\theta = \begin{pmatrix} \sin(\theta) & \cos(\theta) & 0 \\ 0 & 0 & 1 \\ \cos(\theta) & -\sin(\theta) & 0 \end{pmatrix}. \tag{46}$$

The spherical radius vector reads

$$R = \sqrt{r^2 + z^2}.$$

The flux $\mathbf{F}$ and the pressure $\mathbf{P}$ in cylindrical coordinates are written as

$$\mathbf{F} = \begin{pmatrix} F_r \\ F_\varphi \\ F_z \end{pmatrix}, \quad \mathbf{P} = \begin{pmatrix} P_{rr} & P_{r\varphi} & P_{rz} \\ P_{r\varphi} & P_{\varphi\varphi} & P_{\varphi z} \\ P_{rz} & P_{\varphi z} & P_{zz} \end{pmatrix}.$$

In cylindrical coordinates, the model (4) becomes

$$\begin{cases} \partial_t E + \partial_r F_r + \dfrac{F_r}{r} + \partial_z F_z = 0, \\ \dfrac{\epsilon}{c}\partial_t F_r + \dfrac{c}{\epsilon}\partial_r P_{rr} + \dfrac{c}{\epsilon}\partial_z P_{rz} + \dfrac{c}{\epsilon}\dfrac{P_{rr} - P_{\varphi\varphi}}{r} = -\dfrac{\sigma_s}{\epsilon}F_r, \\ \dfrac{\epsilon}{c}\partial_t F_z + \dfrac{c}{\epsilon}\partial_r P_{rz} + \dfrac{c}{\epsilon}\dfrac{P_{rz}}{r} + \dfrac{c}{\epsilon}\partial_z P_{zz} = -\dfrac{\sigma_s}{\epsilon}F_z. \end{cases} \tag{47}$$

The pressure $\mathbf{P}$ and the flux $\mathbf{F}$ are obtained by applying the change of frame $\mathbf{R}_\theta$ to the pressure tensor and the flux of P_1', respectively, expressed in the spherical basis:

$$\mathbf{P} = \mathbf{R}_\theta \begin{pmatrix} P_{RR} & 0 & 0 \\ 0 & P_{\theta\theta} & 0 \\ 0 & 0 & P_{\varphi\varphi} \end{pmatrix} {}^t\mathbf{R}_\theta, \quad \mathbf{F} = \mathbf{R}_\theta \begin{pmatrix} F_R \\ F_\theta \\ F_\varphi \end{pmatrix}, \tag{48}$$

where P_{RR}, $P_{\theta\theta}$ and $P_{\varphi\varphi}$ are defined by (11) and (9), respectively, that is,

$$P_{RR} = \frac{E}{3} + \frac{2\mu_0(R)F_R}{3c}, \quad P_{\theta\theta} = P_{\varphi\varphi} = \frac{E - P_{RR}}{2}, \quad F_R = \sin(\theta)F_r + \cos(\theta)F_z.$$

Hence, we have

$$\mathbf{P} = \begin{pmatrix} \frac{E}{3} + \frac{\mu_0(R)(2\sin(\theta)^2 - \cos(\theta)^2)F_R}{3c} & 0 & \cos(\theta)\sin(\theta)\frac{\mu_0(R)F_R}{c} \\ 0 & \frac{E}{3} - \frac{\mu_0(R)F_R}{3c} & 0 \\ \cos(\theta)\sin(\theta)\frac{\mu_0(R)F_R}{c} & 0 & \frac{E}{3} + \frac{\mu_0(R)(2\cos(\theta)^2 - \sin(\theta)^2)F_R}{3c} \end{pmatrix}, \tag{49}$$

which is the closure relation for the P_1' model in cylindrical coordinates (47).

2.2 Higher order models

This Section introduces the models associated with the structural assumptions (45) and (39). These models are derived in the same manner as P_1', integrating (1) over the unit sphere $\mathcal{S}^2$. They use a larger number of unknowns, hence more equations involving the pressure.

2.2.1 The 3D spherical P_2' model

In this Section, we concentrate on the derivation of a model named P_2' associated with the structural assumption (45). We recall that the final model is expressed in three dimensions because (45) is three dimensional.
The difference between the structural assumptions (45) and (10) is the presence of the first order spherical harmonics in (45). It leads to eight unknowns I_l^m, J_l^m which must be determined using

eight moments. The natural choice of moments would be the eight components of E, $\mathbf{F}$, $\mathbf{P}$. Then the closure would express the third order moment $\mathbf{Q}$ as a function of E, $\mathbf{F}$, $\mathbf{P}$.
However, the moments E, $\mathbf{F}$, $\mathbf{P}$ do not allow to close the system. Indeed, when we compute these moments as functions of the unknowns I_l^m, J_l^m, we get two linear systems of four equations. The moments E, F_R, P_{RR}, $P_{\theta\theta}$ are expressed with the intensities I_0^0, I_1^0, J_0^0, J_1^0 associated with the even spherical harmonics. On the contrary, F_θ, F_φ, $P_{R\theta}$, $P_{R\varphi}$ are expressed with I_1^1, I_1^{-1}, J_1^1, J_1^{-1}. The following lemma asserts that the first linear system is not invertible.

Lemma 2.1 (Relation between E and $\mathbf{P}$)**.** *The structural assumption* (45) *implies that*

$$E = P_{RR} + 2P_{\theta\theta}. \tag{50}$$

Proof. Knowing that $\mathrm{Tr}(\mathbf{P}) = E$, we only need to show that $P_{\theta\theta} = P_{\varphi\varphi}$. This last equality is true because the structural assumption (45) involves only the zeroth and first order spherical harmonics. We have

$$P_{\theta\theta}(t,\mathbf{x}) = \int_{-1}^{1}\int_{0}^{2\pi} (1-\mu^2)\cos(\Phi)^2 I(t,\mathbf{x},\mu,\Phi)d\Phi d\mu.$$

We know that $\cos^2(\Phi)$ is a linear combination of Y_0^0 and Y_2^0. So when I is replaced by (45), we find

$$P_{\theta\theta}(t,\mathbf{x}) = \int_{-1}^{1}\int_{0}^{2\pi} (1-\mu^2)\cos(\Phi)^2 Y_0^0(\Theta,\Phi)\Big(I_0^0(t,\mathbf{x})\mathbb{1}_{-1\leqslant\mu\leqslant\mu_0(R)}(\mu)+J_0^0(t,\mathbf{x})\mathbb{1}_{\mu_0(R)\leqslant\mu\leqslant 1}(\mu)\Big)d\Phi d\mu,$$

by orthogonality of the spherical harmonics basis. A similar argument holds for

$$P_{\varphi\varphi} = \int_{-1}^{1}\int_{0}^{2\pi} (1-\mu^2)\sin(\Phi)^2 Y_0^0(\Theta,\Phi)\Big(I_0^0(t,\mathbf{x})\mathbb{1}_{-1\leqslant\mu\leqslant\mu_0(R)}(\mu) + J_0^0(t,\mathbf{x})\mathbb{1}_{\mu_0(R)\leqslant\mu\leqslant 1}(\mu)\Big)d\Phi d\mu,$$

so that $P_{\theta\theta} = P_{\varphi\varphi}$. □

This issue is a well known problem for the P_n models when n is even [4]. A possible strategy consists in adding a third order moment expressed as a function of $I_0^0, I_1^0, J_0^0, J_1^0$. This expression, together with the equations linking E, F_R, P_{RR} to the corresponding intensities, will form an invertible system. Hence, we choose to replace $P_{\theta\theta}$ by

$$Q_{RRR}(t,\mathbf{x}) = \int_{\mathcal{S}^2} \mu^3 I(t,R,\mathbf{x},\mu,\Phi)d\mu d\Phi,$$

which is the radial component of the third order tensor (14). Thus the model consists of eight equations on $E, F_R, F_\theta, F_\varphi, P_{RR}, P_{R\theta}, P_{R\varphi}, Q_{RRR}$ plus one closure linking the pressures and the energy (50). The equations obtained by integration of (1) over $\mathbf{\Omega}$ (with the scaling relations (16)) are given by

$$
\begin{cases}
\partial_t E + \partial_R F_R + \frac{1}{R}\partial_\theta F_\theta + \frac{1}{R\sin(\theta)}\partial_\varphi F_\varphi + \frac{2}{R}F_R + \frac{\cot(\theta)}{R}F_\theta = 0,\\
\partial_t F_R + \frac{c^2}{\epsilon^2}\partial_R P_{RR} + \frac{c^2}{\epsilon^2 R}\partial_\theta P_{R\theta} + \frac{c^2}{\epsilon^2 R\sin\theta}\partial_\varphi P_{R\varphi} + \frac{c^2}{\epsilon^2 R}\left(2P_{RR} - P_{\theta\theta} - P_{\varphi\varphi}\right) + \frac{c^2\cot\theta}{\epsilon^2 R}P_{R\theta} + \frac{c\sigma_s}{\epsilon^2}F_R = 0,\\
\partial_t F_\theta + \frac{c^2}{\epsilon^2}\partial_R P_{\theta R} + \frac{c^2}{\epsilon^2 R}\partial_\theta P_{\theta\theta} + \frac{c^2}{\epsilon^2 R\sin\theta}\partial_\varphi P_{\theta\varphi} + \frac{3c^2}{\epsilon^2 R}P_{R\theta} + \frac{c^2\cot\theta}{\epsilon^2 R}\left(P_{\theta\theta} - P_{\varphi\varphi}\right) + \frac{c\sigma_s}{\epsilon^2}F_\theta = 0,\\
\partial_t F_\varphi + \frac{c^2}{\epsilon^2}\partial_R P_{\varphi R} + \frac{c^2}{\epsilon^2 R}\partial_\theta P_{\varphi\theta} + \frac{c^2}{\epsilon^2 R\sin\theta}\partial_\varphi P_{\varphi\varphi} + \frac{3c^2}{\epsilon^2 R}P_{R\varphi} + 2\frac{c^2\cot\theta}{\epsilon^2 R}P_{\theta\varphi} + \frac{c\sigma_s}{\epsilon^2}F_\varphi = 0,\\
\partial_t P_{RR} + \partial_R Q_{RRR} + \frac{1}{R}\partial_\theta Q_{RR\theta} + \frac{1}{R\sin(\theta)}\partial_\varphi Q_{RR\varphi} + \frac{2}{R}\left(-F_R + 2Q_{RRR}\right) + \frac{\cot(\theta)}{R}Q_{RR\theta} + \frac{c\sigma_s}{\epsilon^2}\left(P_{RR} - \frac{E}{3}\right) = 0,\\
\partial_t P_{R\theta} + \partial_R Q_{RR\theta} + \frac{1}{R}\partial_\theta Q_{R\theta\theta} + \frac{1}{R\sin(\theta)}\partial_\varphi Q_{R\theta\varphi} + \frac{1}{R}\left(-F_\theta + Q_{RR\theta} + 3Q_{RR\theta}\right) + \frac{\cot(\theta)}{R}\left(Q_{R\theta\theta} - Q_{R\varphi\varphi}\right) + \frac{c\sigma_s}{\epsilon^2}P_{R\theta} = 0,\\
\partial_t P_{R\varphi} + \partial_R Q_{RR\varphi} + \frac{1}{R}\partial_\theta Q_{R\theta\varphi} + \frac{1}{R\sin(\theta)}\partial_\varphi Q_{R\varphi\varphi} + \frac{1}{R}\left(-F_\varphi + 4Q_{RR\varphi}\right) + \frac{2\cot(\theta)}{R}Q_{R\theta\varphi} + \frac{c\sigma_s}{\epsilon^2}P_{R\varphi} = 0,\\
\partial_t P_{\theta\varphi} + \partial_R Q_{R\theta\varphi} + \frac{1}{R}\partial_\theta Q_{\theta\theta\varphi} + \frac{1}{R\sin(\theta)}\partial_\varphi Q_{\theta\varphi\varphi} + \frac{4}{R}Q_{R\theta\varphi} + \frac{\cot(\theta)}{R}\left(2Q_{\theta\theta\varphi} - Q_{\varphi\varphi\varphi}\right) + \frac{c\sigma_s}{\epsilon^2}P_{\theta\varphi} = 0,\\
\frac{\epsilon}{c}\partial_t Q_{RRR} + \partial_R M_{RRRR} + \frac{1}{R}\partial_\theta M_{RRR\theta} + \frac{1}{R\sin(\theta)}\partial_\varphi M_{RRR\varphi} + \frac{1}{R}\left(-3\frac{c}{\epsilon}P_{RR} + 5M_{RRRR}\right) + \frac{\cot(\theta)}{R}M_{RRR\theta} + \frac{c\sigma_s}{\epsilon^2}Q_{RRR} = 0,
\end{cases}
\tag{51}
$$

where $M_{RRRR}, M_{RRR\theta}, M_{RRR\varphi}$ are some components of the fourth order tensor

$$\mathbf{M}(t,\mathbf{x}) = \int_{\mathcal{S}^2} \mathbf{\Omega}\otimes\mathbf{\Omega}\otimes\mathbf{\Omega}\otimes\mathbf{\Omega}\; I(t,\mathbf{x},\mathbf{\Omega})d\mathbf{\Omega}.$$

This system is closed by the relations $P_{\varphi\varphi} = P_{\theta\theta} = (E - P_{RR})/2$. The linear system expressing E, F_R, P_{RR}, Q_{RRR} as a function of $I_0^0, I_1^0, J_0^0, J_1^0$ is now invertible. Computing its solution, one can get the closure

$$
\begin{array}{lll}
Q_{RR\theta} = \frac{4c}{5}\mu_0(R)P_{R\theta} + \frac{1}{5}F_\theta, & Q_{R\theta\theta} = \frac{1}{2}F_R - \frac{1}{2}Q_{RRR}, & Q_{\theta\theta\theta} = -\frac{3c}{5}\mu_0(R)P_{R\theta} + \frac{3}{5}F_\theta,\\
Q_{RR\varphi} = \frac{4c}{5}\mu_0(R)P_{R\varphi} + \frac{1}{5}F_\varphi, & Q_{R\theta\varphi} = 0, & Q_{R\varphi\varphi} = \frac{1}{2}F_R - \frac{1}{2}Q_{RRR},\\
Q_{\theta\theta\varphi} = -\frac{c}{5}\mu_0(R)P_{R\varphi} + \frac{1}{5}F_\varphi, & Q_{\varphi\varphi\varphi} = -\frac{3c}{5}\mu_0(R)P_{R\varphi} + \frac{3}{5}F_\varphi, &\\
Q_{\theta\varphi\varphi} = -\frac{c}{5}\mu_0(R)P_{R\theta} + \frac{1}{5}F_\theta & &
\end{array}
$$

$$
\begin{array}{ll}
M_{RRRR} = \frac{2c}{15}\mu_0(R)^2 E - \frac{2c}{5}\mu_0(R)^2 P_{RR} - \frac{c}{15}E + \frac{4c}{5}P_{RR} - \frac{4}{5}\mu_0(R)F_R + \frac{4}{3}\mu_0(R)Q_{RRR}, &\\
M_{RRR\theta} = \frac{c}{3}(2\mu_0(R)^2 + 1)P_{R\theta}, & M_{RRR\varphi} = \frac{c}{3}(2\mu_0(R)^2 + 1)P_{R\varphi}.
\end{array}
$$

Let us note that this system can degenerate in a bidimensional axisymmetric system. In such a case, $F_\varphi, P_{R\varphi}, P_{\theta\varphi}, Q_{RR\varphi}, Q_{R\theta\varphi}, Q_{\theta\theta\varphi}$ vanish. It amounts to choosing a closure cancelling the odd components of the spherical harmonics of (45), or to expanding on real spherical harmonics.

Finally, let us point out that this model also satisfies the diffusion limit:

Proposition 2.2 (Diffusion limit)**.** *Consider a solution of System* (51)*. Assume E and $\mathbf{F}$ satisfy the following expansion*

$$
\begin{cases}
E = E^{(0)} + \epsilon E^{(1)} + \mathcal{O}(\epsilon^2),\\
\mathbf{F} = \mathbf{F}^{(0)} + \epsilon \mathbf{F}^{(1)} + \mathcal{O}(\epsilon^2),
\end{cases}
\tag{52}
$$

as ϵ goes to 0, and similarly for $\mathbf{P}$ and $\mathbf{Q}$. Then $E^{(0)}$ is a solution to

$$\partial_t E^{(0)} - \operatorname{div}\Big(\frac{c}{3\sigma_s}\nabla E^{(0)}\Big) = 0. \tag{53}$$

Proof. Here again, as in Proposition 1.3, we only give a formal proof. A rigorous proof may easily be derived using the methods in [17]. Inserting (52) into the first line of (51) and identifying the powers of ϵ, one gets

$$\partial_t E^{(0)} + \partial_R F_R^{(0)} + \frac{1}{R}\partial_\theta F_\theta^{(0)} + \frac{1}{R\sin(\theta)}\partial_\varphi F_\varphi^{(0)} + \frac{2}{R}F_R^{(0)} + \frac{\cot(\theta)}{R}F_\theta^{(0)} = 0,$$

that is,

$$\partial_t E^{(0)} + \operatorname{div}\left(\mathbf{F}^{(0)}\right) = 0. \tag{54}$$

Next, we insert the expansion into the second, third and fourth equations of (51). This easily gives

$$\mathbf{F}^{(0)} = -\frac{c}{\sigma_s}\operatorname{div}\left(\mathbf{P}^{(0)}\right).$$

Now, equations five to eight in System (51) imply that

$$P_{RR}^{(0)} = \frac{E}{3}, \quad P_{R\theta}^{(0)} = P_{R\varphi}^{(0)} = P_{\theta\varphi}^{(0)} = 0.$$

Hence, since we also have $P_{\theta\theta} = P_{\varphi\varphi} = (E - P_{RR})/2$, we infer

$$\mathbf{P}^{(0)} = \frac{E}{3}\begin{pmatrix} 1 & 0 & 0 \\ 0 & 1 & 0 \\ 0 & 0 & 1 \end{pmatrix}, \quad \text{whence} \quad \mathbf{F}^{(0)} = -\frac{c}{3\sigma_s}\nabla E^{(0)}.$$

Inserting this equation into (54), we find (53). □

2.2.2 The cylindrical P_2' model

This paragraph aims at taking into account the cylindrical symmetry contrary to the P_2' three dimensional model (Section 2.2.1). We choose to derive it in spherical coordinates. It can be written in cylindrical coordinates using the change of variables defined by (46) and (48). The idea originates from the P_1' model which preserves the radially symmetric stationary solutions of the radiative transfer equation (1) in pure transport (Section 1.3). For $\sigma_s = 0$, given a boundary condition

$$I(R_2, \theta, \varphi, \mathbf{\Omega}) = P_l(\cos(\theta)), \quad l \in \{0, 1, 2\},$$

the solution of our future model must be equal to the radiative transfer equation solution. (Note that the P_1' model achieves this for $l = 0$.) This solution can be explicitly obtained with the method of characteristics. Thus, the intensity (39) at the point $M = (R, \theta, \varphi)$ in the direction $\mathbf{\Omega}$ is the same as at the point M': $I(M, \mathbf{\Omega}) = P_2(\cos(\theta'(\mathbf{\Omega})))$ (see Figure 6).
This is why we choose the structural assumption (39) taking into account both these exact solutions and the shadow cone. This structural assumption involves six unknowns I_l, J_l, $l \in \{0, 1, 2\}$. Hence, six moments are needed to determine these unknowns: $E, F_R, F_\theta, P_{RR}, P_{R\theta}, P_{\theta\theta}$. Applied to the

axisymmetric intensity (39), $F_\varphi, P_{R\varphi}, P_{\theta\varphi}$ vanish. The general equations of the model are given by (47) written in spherical coordinates plus the equations on the pressure, with, here again, the scaling law (16):

$$\begin{cases} \partial_t E + \partial_R F_R + \dfrac{1}{R}\partial_\theta F_\theta + \dfrac{2}{R}F_R + \dfrac{\cot(\theta)}{R}F_\theta = 0, \\ \partial_t F_R + \dfrac{c^2}{\epsilon^2}\partial_R P_{RR} + \dfrac{c^2}{\epsilon^2 R}\partial_\theta P_{R\theta} + \dfrac{c^2}{\epsilon^2 R}\left(2P_{RR} - P_{\theta\theta} - P_{\varphi\varphi}\right) + \dfrac{c^2\cot\theta}{\epsilon^2 R}P_{R\theta} + \dfrac{c\sigma_s}{\epsilon^2}F_R = 0, \\ \partial_t F_\theta + \dfrac{c^2}{\epsilon^2}\partial_R P_{\theta R} + \dfrac{c^2}{\epsilon^2 R}\partial_\theta P_{\theta\theta} + \dfrac{3c^2}{\epsilon^2 R}P_{R\theta} + \dfrac{c^2\cot\theta}{\epsilon^2 R}\left(P_{\theta\theta} - P_{\varphi\varphi}\right) + \dfrac{c\sigma_s}{\epsilon^2}F_\theta = 0, \\ \partial_t P_{RR} + \partial_R Q_{RRR} + \dfrac{1}{R}\partial_\theta Q_{RR\theta} + \dfrac{2}{R}\left(-F_R + 2Q_{RRR}\right) + \dfrac{\cot(\theta)}{R}Q_{RR\theta} + \dfrac{c\sigma_s}{\epsilon^2}\left(P_{RR} - \dfrac{E}{3}\right) = 0, \\ \partial_t P_{R\theta} + \partial_R Q_{RR\theta} + \dfrac{1}{R}\partial_\theta Q_{R\theta\theta} + \dfrac{1}{R}\left(-F_\theta + Q_{RR\theta} + 3Q_{RR\theta}\right) + \dfrac{\cot(\theta)}{R}\left(Q_{R\theta\theta} - Q_{R\varphi\varphi}\right) + \dfrac{c\sigma_s}{\epsilon^2}P_{R\theta} = 0, \\ \partial_t P_{\theta\theta} + \partial_R Q_{R\theta\theta} + \dfrac{1}{R}Q_{\theta\theta\theta} + \dfrac{4}{R}Q_{R\theta\theta} + \dfrac{\cot\theta}{R}\left(Q_{\theta\theta\theta} - 2Q_{\varphi\varphi\theta}\right) + \dfrac{c\sigma_s}{\epsilon^2}\left(P_{\theta\theta} - \dfrac{E}{3}\right) = 0. \end{cases} \tag{55}$$

To close the system, we need an expression of the third order tensor $\mathbf{Q}$ as a function of the lower order moments $E, F_R, F_\theta, P_{RR}, P_{R\theta}, P_{\theta\theta}$. To get $\mathbf{Q}$, the six moments $Q_{RRR}, Q_{RR\theta}, Q_{R\theta\theta}, Q_{R\varphi\varphi}, Q_{\theta\theta\theta}, Q_{\theta\varphi\varphi}$ are evaluated as an invertible linear system on the six unknowns I_l, J_l. To do so, we integrate (39) against

$$1,\ \mu,\ \sqrt{1-\mu^2}\cos(\Phi),\ \mu^2,\ \mu\sqrt{1-\mu^2}\cos(\Phi),\ (1-\mu^2)\cos(\Phi)^2.$$

This leads to the computation of the integrals

$$\frac{1}{c}\int_{-1}^{\mu_0(R)}\int_0^{2\pi} P(\mathbf{\Omega}(\mu,\Phi))P_l(\cos(\theta'(\mathbf{\Omega})))d\mu d\Phi,$$

$$\frac{1}{c}\int_{\mu_0(R)}^{1}\int_0^{2\pi} P(\mathbf{\Omega}(\mu,\Phi))P_l(\cos(\theta'(\mathbf{\Omega})))d\mu d\Phi,$$

where $\mathbf{\Omega}(\mu,\Phi) = (\mu, \sqrt{1-\mu^2}\cos(\Phi), \sqrt{1-\mu^2}\sin(\Phi))$. If μ_0 is given by Formula (13), that is, $\mu_0(R) = \sqrt{1-R_1^2/R^2}$, these integrals are similar to (34). We have seen that they are computable with two variable changes but this computation is cumbersome. Then the inversion of the linear system cannot be computed analytically. So the closure needs to be numerically evaluated at each time step. Finally, going back to cylindrical coordinates is made using the change of coordinates (46) and (48).

Note that the linear system is expected to be invertible contrary to the spherical harmonics case (Section 2.2.1). Indeed, Assumption (39) involves second order Legendre polynomials hence second order spherical harmonics. So Relation (50), which prevents the system from being invertible, is no longer valid.

As before, one easily proves that this model satisfies the diffusion limit.

Proposition 2.3 (Diffusion limit)**.** *Consider a solution of the system* (55)*. Assume E and $\mathbf{F}$ satisfy the expansions given by* (52) *as ϵ goes to* 0*, and similarly for $\mathbf{P}$ and $\mathbf{Q}$. Then $E^{(0)}$ is a solution to*

$$\partial_t E^{(0)} - \operatorname{div}\Big(\frac{c}{3\sigma_s}\nabla E^{(0)}\Big) = 0.$$

2.2.3 Calculation of μ_0

This paragraph briefly explains a possible way to compute μ_0. We have already mentioned about the method of [42] for the P_1' model, consisting in adding an equation on the pressure (Section 1.1). The radial symmetry of P_1' allows simplifications that do not occur in a more complex model. However, it is possible to turn this into a numerical strategy. Here again, we add an equation on an additional moment: all the moments are then expressed with the lower order moments and μ_0 thanks to the closure. At each time step, we use the moments $E^n, \mathbf{F}^n$, etc... from the preceding time step, to solve the equation satisfied by μ_0. This gives μ_0^n, an approximation of $\mu_0(t^n)$, which may be used to compute the radiative moments at time t^{n+1}.

3 Asymptotic preserving discretization of the P_1' model in the radial case

As already told, the numerics of this contribution are restricted to the one dimensional radially symmetric case: this Section focuses on with the numerical discretization of the P_1' model. However, this framework may be useful to derive schemes for the models presented above.
The purpose of this Section is to design a precise scheme in both transport ($\sigma_s = 0$) and diffusion regimes ($\sigma_s \to \infty$, $c \to \infty$). We want the scheme to reproduce the diffusion limit (7) as σ_s and c tend to infinity. In other words, we need to derive a so called asymptotic preserving scheme. A rather natural way to achieve this is to use discontinuous Galerkin discretization, as for instance in [28]. However, in ICF applications we consider here, the radiation transfer equation (1) is coupled to a Lagragian hydrodynamics scheme which is usually of finite volume type. Therefore, in order to simplify this coupling, we prefer considering finite volume scheme for the P_1' model.
In the one dimensional cartesian framework, a large literature exists on asymptotic preserving schemes. Let us for instance cite the former work of Jin and Levermore [27], in which the sources are inserted in the flux, the splitting methods [25] and the well-balanced methods [20, 21]. Other methods, based on Godunov type fluxes were proposed in [2, 3]. A full review of such methods is beyond the scope of this article, and the interested reader is referred to the reviews [24, 26]. The design of well-balanced scheme needs a careful discretization of the stationary solutions, hence of the interplay between flux and source terms. Moreover, when preservation of an equilibrium state is related to the asymptotic limit of the model, the design of well-balanced schemes may be a good way to build asymptotic-preserving schemes. It is the case of the P_1' model: in the diffusion limit, we have

$$F_R^{(0)} = -\frac{c}{3\sigma_s(R)}\partial_R E^0 \tag{56}$$

where $E^{(0)}$ and $F_R^{(0)}$ are the zero-th order terms of E and F_R in the Chapman-Enskog expansion (see Section 1.2).
In the case of spherical or cylindrical geometries, few works deal with asymptotic preserving schemes. In [43], a discretization of P_n models is proposed for the one dimensional radial geometry while [35] studies the numerical resolution of the P_1 model for a two dimensional cylindrical geometry.
A well-balanced strategy has however been proposed by Buet and Després [9] which could be used in the one dimensional radial geometry. It is well-suited to linear hyperbolic systems of Friedrichs type with linear relaxation terms. This method transforms a linear hyperbolic system in an equivalent conservative homogeneous formulation which is the starting point of the discretization. This method

has been adapted to the P_n closure in the one dimensional radial geometry [43]. We use it to derive an asymptotic preserving scheme for the P_1' model. We compare it to a staggered method which is one of the simplest way to get an asymptotic preserving scheme. This staggered scheme is asymptotic preserving but may produce oscillations in the transport regime (σ_s small) for non smooth solutions. We hope that the Buet-Després scheme has a nicer behavior in this regime.

3.1 General framework

In this Section, we give some general notations and definitions we use. We first introduce the mesh notations. Let $[a, b]$ be a given interval of $\mathbb{R}$ discretized by a regular grid of N cells. The center of the i^{th} cell is the R_i point and the grid interfaces are located at the nodes $R_{i\pm\frac{1}{2}}$ such that

$$R_{i+\frac{1}{2}} = R_{i-\frac{1}{2}} + \Delta R_i,$$

with ΔR_i the mesh step. Moreover, we define the global mesh step by

$$\Delta R = \min_{1 \leqslant i \leqslant N} \Delta R_i.$$

Let $[0, T]$ be the time interval. It is discretized by a uniform mesh associated with the time step Δt: $t^n = n\Delta t$.

Let us now introduce some definitions.

Definition 3.1. *A scheme consistent with the P_1' model is said to be well-balanced if it preserves exactly the stationary solutions of this model at every time t^n, $n \in \mathbb{N}$.*

Definition 3.2. *[25, 6] Let $\mathcal{P}^{\epsilon}_{\Delta R_i}$ be a discretization of the P_1' model* (19).
If the scheme $\mathcal{P}^{0}_{\Delta R_i}$ is consistent with the diffusion equation (27)*, then it is said to be asymptotic preserving.*

Definition 3.3. *Let $\mathcal{P}^{\epsilon}_{\Delta R_i}$ be a scheme consistent with the P_1' model* (19) *as ΔR_i goes to 0 at a given order.*
The scheme $\mathcal{P}^{\epsilon}_{\Delta R_i}$ is said to be asymptotically stable if the stability condition does not tend to $\Delta t = 0$ as ϵ goes to 0.

3.2 Staggered scheme

This paragraph presents an asymptotic preserving staggered scheme. The staggered scheme [17] is one of the simplest way to capture the diffusion limit. In such a scheme, some of the unknowns are constant over the cell i and the other ones are constant over the dual cell $[R_i, R_{i+1}]$. For the P_1' model, the energy E is assumed to be constant over the cells and the flux F_R over the dual cells. Hence, a staggered scheme for the P_1' model can be derived by a finite volume integration of the first equation of (19) on the i^{th} cell $[R_{i-\frac{1}{2}}, R_{i+\frac{1}{2}}]$ and a finite volume integration of the second equation of (19) on the dual cell $[R_i, R_{i+1}]$. This gives, in the implicit case,

$$\left\{\begin{array}{l} V_i\,\dfrac{E_i^{n+1}-E_i^n}{\Delta t}+\Big(S_{i+\frac12}F_{i+\frac12}^{n+1}-S_{i-\frac12}F_{i-\frac12}^{n+1}\Big)=0,\\[2ex] V_{i+\frac12}\,\dfrac{F_{i+\frac12}^{n+1}-F_{i+\frac12}^n}{\Delta t}+\dfrac{c}{3\epsilon}S_{i+\frac12}\left[\dfrac{c}{\epsilon}(E_{i+1}^{n+1}-E_i^{n+1})+2\Big(\mu_0(R_{i+1})F_{i+1}^{n+1}-\mu_0(R_i)F_i^{n+1}\Big)\right]\\ \qquad\qquad +2\,\dfrac{c\,V_{i+\frac12}}{\epsilon\,R_{i+\frac12}}\mu_0(R_{i+\frac12})F_{i+\frac12}^{n+1}+\dfrac{c}{\epsilon^2}V_{i+\frac12}\,\sigma_s(R_{i+\frac12})F_{i+\frac12}^{n+1}=0, \end{array}\right.$$

while, in the explicit case, we have

$$\left\{\begin{array}{l} V_i\,\dfrac{E_i^{n+1}-E_i^n}{\Delta t}+\Big(S_{i+\frac12}F_{i+\frac12}^{n}-S_{i-\frac12}F_{i-\frac12}^{n}\Big)=0,\\[2ex] V_{i+\frac12}\,\dfrac{F_{i+\frac12}^{n+1}-F_{i+\frac12}^n}{\Delta t}+\dfrac{c}{3\epsilon}S_{i+\frac12}\left[\dfrac{c}{\epsilon}(E_{i+1}^{n}-E_i^{n})+2\Big(\mu_0(R_{i+1})F_{i+1}^{n}-\mu_0(R_i)F_i^{n}\Big)\right]\\ \qquad\qquad +2\,\dfrac{c\,V_{i+\frac12}}{\epsilon\,R_{i+\frac12}}\mu_0(R_{i+\frac12})F_{i+\frac12}^{n}+\dfrac{c}{\epsilon^2}V_{i+\frac12}\,\sigma_s(R_{i+\frac12})F_{i+\frac12}^{n}=0, \end{array}\right.$$

where V_i denotes the volume of the cell i, $V_{i+\frac12}=\dfrac{4}{3}\pi\left(R_{i+1}^3-R_i^3\right)$ the volume of the annulus included between R_i and R_{i+1}. The quantity $S_{i+\frac12}$ is the surface calculated at the node $R_{i+\frac12}$. The flux at the center of the cell is defined by

$$F_i^{n+1}=\frac{F_{i+\frac12}^{n+1}+F_{i-\frac12}^{n+1}}{2}\,.$$

We can obtain the limit scheme doing a Chapman-Enskog expansion as in Section 1.2. The limit scheme reads (in the implicit case)

$$V_i\,\frac{E_i^{n+1,(0)}-E_i^{n,(0)}}{\Delta t}-\frac{c}{3}\left[S_{i+\frac12}^2\frac{E_{i+1}^{n+1,(0)}-E_i^{n+1,(0)}}{\sigma_s(R_{i+\frac12})V_{i+\frac12}}-S_{i-\frac12}^2\frac{E_i^{n+1,(0)}-E_{i-1}^{n+1,(0)}}{\sigma_s(R_{i-\frac12})V_{i-\frac12}}\right]=0.$$

In the explicit case, it reads

$$V_i\,\frac{E_i^{n+1,(0)}-E_i^{n,(0)}}{\Delta t}-\frac{c}{3}\left[S_{i+\frac12}^2\frac{E_{i+1}^{n,(0)}-E_i^{n,(0)}}{\sigma_s(R_{i+\frac12})V_{i+\frac12}}-S_{i-\frac12}^2\frac{E_i^{n,(0)}-E_{i-1}^{n,(0)}}{\sigma_s(R_{i-\frac12})V_{i-\frac12}}\right]=0.$$

It is consistent with the diffusion equation (27) as the space and time steps tend to zero.
In spite of its simplicity, this scheme has some drawbacks we want to avoid. The first one is related to the stability condition: we want the scheme to be asymptotically stable in the diffusion regime, in the sense of Definition 3.3. The explicit staggered scheme (as the following Buet-Després scheme) is stable under a condition of the kind $\Delta t\leqslant C\epsilon\Delta R$ which becomes too restrictive when ϵ tends to 0. Hence, an implicit version of the scheme must be used to get a stability condition independent of ϵ in the diffusion regime. This implicitation requires the inversion of a linear system. The second drawback of the staggered scheme is illustrated on the Figure 10: it may produce oscillations in the transport regime (σ_s small). This is a problem since the applications we have in mind imply both transport and diffusion. Hence, we need a methodology which is precise in both regimes.

3.3 A partially implicit Buet-Després type scheme

In this paragraph, we use the Buet-Després methodology [9] introduced to build well-balanced schemes. Our hope is that, as in [9], applying this method, we find an asymptotic preserving scheme consistent with the P_1' model. A scheme is derived for this model and its properties are discussed. We use a partially implicit discretization of some terms so as to have an asymptotical stability in the diffusion regime ($\epsilon \to 0$).
The initial framework [9] was developed for linear Friedrichs systems having stationary states and a linear relaxation term. Here, we apply it to the P_1' model which is such a system.
The key idea is to build the scheme from a homogeneous conservative formulation equivalent to the initial model. Starting from a homogeneous conservative formulation is a natural way to build well-balanced and asymptotic preserving schemes in one dimension. As already pointed out above, the equilibrium states are intimately linked with the diffusion limit, as (56) shows. This is why we use this method to derive our asymptotic preserving scheme.

3.3.1 A homogeneous conservative formulation of the P_1' model

Wanting to apply the method of [9], we consider the P_1' model written as (20), (21), and write its dual system:

$$\partial_t \mathbf{V} + \frac{1}{\epsilon} {}^t\mathbf{A}(R)\partial_R \mathbf{V} = -\frac{1}{\epsilon} {}^t\mathbf{G}_\epsilon(R)\mathbf{V}.$$

If $\mathbf{U}$ and $\mathbf{V}$ are solutions of the primal and the dual systems, they satisfy the following homogeneous conservative equation

$$\partial_t \left(\mathbf{U}\cdot\mathbf{V}\right) + \frac{1}{R^2\epsilon}\partial_R\Big(R^2\left(\mathbf{A}(R)\mathbf{U}\cdot\mathbf{V}\right)\Big) = 0,$$

where $\cdot$ is the canonical scalar product of $\mathbb{R}^p, p \in \mathbb{N}$. Then given a basis of solutions of this dual system, one can form a homogeneous conservative system of equations equivalent to P_1'. The one dimensional framework is a real advantage to exhibit such a basis. The stationary dual equation is thus a linear system of ordinary differential equations

$$\partial_R \mathbf{V} = -\mathbf{A}(R)^{-1}\ {}^t\mathbf{G}_\epsilon(R)\mathbf{V} = \begin{pmatrix} 0 & \frac{\sqrt{3}}{R\epsilon}(R\sigma_s(R) + 2\epsilon\mu_0(R)) \\ 0 & -\frac{2}{R} \end{pmatrix}\mathbf{V}.$$

Since $\mathbf{A}(R)$ is invertible, this system has a unique solution for any boundary condition at $R = R_0 > 0$. We get a two dimensional vector space of solutions given by $\mathbf{V}_i = (V_{i,1}, V_{i,2}) \in \mathbb{R}^2$, $i = 1, 2$,

$$V_{i,1} = C_{i,2} + C_{i,1}\int_{R_0}^{R} \frac{\sqrt{3}}{u^3\epsilon}(u\sigma_s(u) + 2\epsilon\mu_0(u))du, \quad V_{i,2} = \frac{C_{i,1}}{R^2},$$

for $C_{i,1}, C_{i,2}, R_0$ some real constants. Taking successively $(C_{i,1}, C_{i,2}) = (0, 1)$ and $(C_{i,1}, C_{i,2}) = (1, 0)$, we obtain two solutions

$$\mathbf{V}_1 = (1, 0), \quad \mathbf{V}_2 = (f_\epsilon(R), \tfrac{1}{R^2}),$$

where

$$f_\epsilon(R) = \int_{R_0}^{R} \frac{\sqrt{3}}{u^3\epsilon}(u\sigma_s(u) + 2\epsilon\mu_0(u))du. \tag{57}$$

Since the integrand of (57) is non-negative, f_ϵ is a non-decreasing function of R. The new system of conservation laws is given by

$$\partial_t \left(\mathbf{U}\cdot\mathbf{V}_i\right) + \frac{1}{R^2\epsilon}\partial_R\Big(R^2\left(\mathbf{A}(R)\mathbf{U}\cdot\mathbf{V}_i\right)\Big) = 0, \quad i=1,2. \tag{58}$$

The new variable $\mathbf{W}_\epsilon = \left(\left(\mathbf{U}\cdot\mathbf{V}_1\right), \left(\mathbf{U}\cdot\mathbf{V}_2\right)\right)$ satisfies

$$\mathbf{W}_\epsilon = \mathbf{V}_\epsilon \mathbf{U}, \tag{59}$$

where

$$\mathbf{V}_\epsilon(R) = \begin{pmatrix} 1 & 0 \\ f_\epsilon(R) & \frac{1}{R^2} \end{pmatrix}.$$

Then the hyperbolic system (58) writes equivalently as

$$\partial_t \mathbf{W}_\epsilon + \frac{1}{\epsilon R^2}\partial_R(R^2\mathbf{B}_\epsilon(R)\mathbf{W}_\epsilon) = 0, \tag{60}$$

with $\mathbf{B}_\epsilon = \mathbf{V}_\epsilon \mathbf{A}(\mathbf{V}_\epsilon)^{-1}$. This model is the starting point of the discretization.

3.3.2 Explicit Buet-Després type scheme

This paragraph presents an explicit discretization of the system (60). A finite volume method is applied; the system being linear, the spatial discretization is based on the resolution of Riemann problems with an upwind method. Let us denote $\mathbf{W}_i^n$ the mean of $\mathbf{W}_\epsilon$ on each cell $[R_{i-\frac{1}{2}}, R_{i+\frac{1}{2}}]$

$$\mathbf{W}_i^n = \frac{1}{V_i}\int_{R_{i-\frac{1}{2}}}^{R_{i+\frac{1}{2}}} \mathbf{W}_\epsilon(t^n, R)\, 4\pi R^2 dR.$$

After integrating (60) over the cell $[R_{i-\frac{1}{2}}, R_{i+\frac{1}{2}}]$, we get the general finite volume scheme

$$\frac{\mathbf{W}_i^{n+1}-\mathbf{W}_i^n}{\Delta t} + \frac{1}{\epsilon V_i}\Big((4\pi R^2\mathbf{B}_\epsilon\mathbf{W}_\epsilon)_{i+\frac{1}{2}}^n - (4\pi R^2\mathbf{B}_\epsilon\mathbf{W}_\epsilon)_{i-\frac{1}{2}}^n\Big) = 0. \tag{61}$$

Next, we need to evaluate the fluxes at the nodes. To do so, we use an upwind discretization as in [9]. The first step consists in considering the variable

$$\mathbf{Z} = R^2\mathbf{B}_\epsilon(R)\mathbf{W}_\epsilon \tag{62}$$

satisfying the cartesian hyperbolic system with a space dependent flux

$$\partial_t\mathbf{Z} + \frac{1}{\epsilon}\mathbf{B}_\epsilon(R)\partial_R\mathbf{Z} = 0. \tag{63}$$

The upwind method requires the diagonalization of the matrix $\mathbf{B}_\epsilon(R)$. Following Buet and Després [9], the matrix $\mathbf{B}_\epsilon(R)$ is approximated by a piecewise constant function in each cell $[R_{i-\frac{1}{2}}, R_{i+\frac{1}{2}}]$

$$\mathbf{B}_\epsilon(R) = \begin{cases} \mathbf{B}_\epsilon(R_i) & \text{if } R_i \leqslant R \leqslant R_{i+\frac{1}{2}}, \\ \mathbf{B}_\epsilon(R_{i+1}) & \text{if } R_{i+\frac{1}{2}} \leqslant R \leqslant R_{i+1}. \end{cases}$$

The matrices $\mathbf{B}_\epsilon$ and $\mathbf{A}$ being similar, the eigenvalues of the matrix $\mathbf{B}_\epsilon$ are given by (24). Let us note $\mathbf{P}_\epsilon$ the matrix of the right eigenvectors of $\mathbf{B}_\epsilon$, $\mathcal{L}_i^+$ the left eigenvector associated with λ^+ at R_i and $\mathcal{L}_{i+1}^-$ the left eigenvector associated with λ^- at R_{i+1}. They satisfy

$$\begin{cases} \mathcal{L}_i^+ = (\mathbf{P}_\epsilon(R_i)^{-1})_{1:} \\ \mathcal{L}_{i+1}^- = (\mathbf{P}_\epsilon(R_{i+1})^{-1})_{2:} \end{cases}$$

where $(M)_{k:}$ denotes the k^{th} row of a given matrix M.
Then the upwind method reads

$$\begin{cases} (\mathcal{L}_i^+ \cdot \mathbf{Z}_{i+\frac{1}{2}}) = \left(\mathcal{L}_i^+ \cdot \mathbf{Z}_i\right), \\ (\mathcal{L}_{i+1}^- \cdot \mathbf{Z}_{i+\frac{1}{2}}) = \left(\mathcal{L}_{i+1}^- \cdot \mathbf{Z}_{i+1}\right). \end{cases}$$

The inversion of this linear system gives:

$$\begin{cases} (Z_1)_{i+\frac{1}{2}}^n = \dfrac{\lambda_i^+ R_i^2 x_{i+1}^- Z_{1,i+1}^n - \lambda_{i+1}^- R_{i+1}^2 x_i^+ Z_{1,i}^n + \frac{\sqrt{3}}{c}\lambda_i^+\lambda_{i+1}^- R_i^2 R_{i+1}^2 (Z_{2,i+1}^n - Z_{2,i}^n)}{\lambda_i^+ R_i^2 x_{i+1}^- - \lambda_{i+1}^- R_{i+1}^2 x_i^+} \\ (Z_2)_{i+\frac{1}{2}}^n = \dfrac{\lambda_i^+ R_i^2 x_{i+1}^- Z_{2,i}^n - \lambda_{i+1}^- R_{i+1}^2 x_i^+ Z_{2,i+1}^n - \frac{c}{\sqrt{3}} x_i^+ x_{i+1}^- (Z_{1,i+1}^n - Z_{1,i}^n)}{\lambda_i^+ R_i^2 x_{i+1}^- - \lambda_{i+1}^- R_{i+1}^2 x_i^+} \end{cases} \tag{64}$$

where $\lambda_i^\pm$, $f_{\epsilon,i}$ denote $\lambda^\pm(R_i)$, $f_\epsilon(R_i)$ and

$$x_i^\pm = 1 - \frac{\sqrt{3}}{c}\lambda_i^\pm f_{\epsilon,i} R_i^2.$$

The scheme on $\mathbf{W}_\epsilon$ is then obtained by inserting the relation (62) $\mathbf{Z}_{i+\frac{1}{2}}^n = \left(R^2 \mathbf{B}_\epsilon(R) \mathbf{W}_\epsilon{}^n\right)_{i+\frac{1}{2}}$ in the finite volume formulation (61).
Then the scheme on the primal variables E, F_R is easily obtained with the change of frame (59).

Let us make some remarks on the scheme (61)-(62)-(64).
First, this scheme is well defined because the denominator involved in the relations (64) never vanishes. Indeed, it is the sum of two positive terms

$$\lambda_i^+ R_i^2 x_{i+1}^- - \lambda_{i+1}^- R_{i+1}^2 x_i^+ = \left(\lambda_i^+ R_i^2 - \lambda_{i+1}^- R_{i+1}^2\right) + \frac{\sqrt{3}}{c}\lambda_i^+\lambda_{i+1}^- R_i^2 R_{i+1}^2 \left(f_{\epsilon,i} - f_{\epsilon,i+1}\right)$$

as $\lambda^-(R) < 0 < \lambda^+(R)$ and f_ϵ is an increasing function of R.
Second, this scheme can ensure a zero flux boundary condition at $R = 0$, which is the natural boundary condition for a one dimensional radial geometry at $R = 0$.

Remark 3.4. *The numerical fluxes* (64) *can be written as functions of the cartesian Riemann invariants* (25) *multiplied by* R^2. *Let us note*

$$\omega^\pm(R) = R^2\Big(cE(R) + \epsilon\frac{3}{c}\lambda^\mp(R) F_R(R)\Big), \quad \omega_i^\pm = \omega^\pm(R_i).$$

Then, the numerical fluxes are given by

$$\begin{cases} (Z_1)^n_{i+\frac{1}{2}} = -\dfrac{c}{\epsilon\sqrt{3}D^n_i}\Big((R_{i+1})^2\omega^{-,\,n}_i - (R_i)^2\omega^{+,\,n}_{i+1}\Big) \\ (Z_2)^n_{i+\frac{1}{2}} = -\dfrac{c}{3\epsilon D^n_i}\omega^{-,n}_i\Big(\dfrac{3}{c}\lambda^+_{i+1} + \sqrt{3}(R_{i+1})^2 f_{\epsilon,i+1}\Big) + \dfrac{c}{3\epsilon D^n_i}\omega^{+,n}_{i+1}\Big(\dfrac{3}{c}\lambda^-_i + \sqrt{3}(R_i)^2 f_{\epsilon,i}\Big), \end{cases}$$

and

$$D^n_i = -\frac{3}{c}\big((R_i)^2\lambda^+_{i+1} - (R_{i+1})^2\lambda^-_i\big) + \sqrt{3}(R_i)^2(R_{i+1})^2\big(f_{\epsilon,i} - f_{\epsilon,i+1}\big).$$

The explicit Buet-Després type scheme (61)-(62)-(64), written for the P_1 model ($\mu_0 = 0$) and an arbitrary $\sigma_s(R)$, reads

$$E^{n+1}_i = \big(1 - a^+_i - a^-_i\big)\,E^n_i + a^+_i E^n_{i+1} + a^-_i E^n_{i-1} + \frac{\epsilon\sqrt{3}}{c}\left[\big(a^-_i - a^+_i\big)\,F^n_i - a^+_i F^n_{i+1} + a^-_i F^n_{i-1}\right], \quad (65)$$

$$F^{n+1}_i = \frac{c}{\epsilon\sqrt{3}}\left[\big(a^+_i - a^-_i\big)\,E^n_i - a^+_i E^n_{i+1} + a^-_i E^n_{i-1}\right] + (1-b_i)F^n_i + a^+_i F^n_{i+1} + a^-_i F^n_{i-1}, \quad (66)$$

where

$$a^\pm_i = \frac{4\pi c\Delta t}{V_i\sqrt{3}}\frac{R^2_i R^2_{i\pm1}}{\epsilon\left(R^2_i + R^2_{i\pm1}\right) + R^2_i R^2_{i\pm1}\epsilon\Delta f_{i\pm\frac{1}{2}}}, \quad (67)$$

$$b_i = \left(\frac{R^2_i}{R^2_{i+1}} + R^2_i\Delta f_{i+\frac{1}{2}}\right)a^+_i + \left(\frac{R^2_i}{R^2_{i-1}} + R^2_i\Delta f_{i-\frac{1}{2}}\right)a^-_i, \quad (68)$$

$$\epsilon\Delta f_{i\pm\frac{1}{2}} = 4\sqrt{3}\sigma_s(R_{i\pm\frac{1}{2}})\frac{|R_{i\pm1} - R_i|}{(R_i + R_{i\pm1})^2}, \quad (69)$$

It should be noted that the above coefficients satisfy

$$b_i + a^+_i + a^-_i = \frac{4\pi c\Delta t}{V_i\sqrt{3}}\frac{2R^2_i}{\epsilon}. \quad (70)$$

In order to obtain the above expressions, we have used a quadrature method in order to compute $f_i = f_\epsilon(R_i)$, which is defined as an integral (57). Here, we have used a trapezoidal rule.

Remark 3.5. *We would like to relate the present scheme to the one presented in [43, page 48] for the P_1 (that is, $\mu_0 = 0$) model. Actually, scheme of [43] is equivalent to the present one if we have*

$$\frac{4\pi R^2_i}{V_i} = \frac{1}{\Delta R_i}, \quad (71)$$

$$\Delta f_{i\pm\frac{1}{2}} = \frac{\sqrt{3}}{\epsilon}\left(\pm\sigma_s(R_i)\left(\frac{1}{R_i} - \frac{1}{R_{i\pm\frac{1}{2}}}\right) \pm \sigma_s(R_{i\pm1})\left(\frac{1}{R_{i\pm\frac{1}{2}}} - \frac{1}{R_{i\pm1}}\right)\right), \quad (72)$$

Relation (71) *is exact up to second-order terms in ΔR_i, as shows* (80) *below. On the other hand,* (72) *is a particular quadrature formula. A way to obtain it corresponds to assuming that σ_s is*

piecewise constant in the interval $[R_i, R_{i+1}]$*, with value* $\sigma_s(R_i)$ *in* $\left[R_i, R_{i+\frac{1}{2}}\right]$ *and* $\sigma_s(R_{i+1})$ *in* $\left[R_{i+\frac{1}{2}}, R_{i+1}\right]$*. Thus, this is only a first-order quadrature formula. Nevertheless, it should be noted that if* σ_s *is constant, this quadrature formula is exact, and thus we recover the present scheme, up to* (71)*. Since the scheme proposed in [43] is written in finite volume form, this indicates that* (65)-(66)-(67)-(68)-(69)-(70) *below may be written in finite volume form, although this is not clear in the expressions* (65)-(66)*.*

In the case $\mu_0 \neq 0$, it is also possible to write the scheme in the same form. An easy but tedious computation gives

$$E_i^{n+1} = \left(1 - a_i^+ - a_i^-\right) E_i^n + a_i^+ E_{i+1}^n + a_i^- E_{i-1}^n + \frac{3\epsilon}{c^2}\left[\lambda_{i+1}^- a_i^+ F_{i+1}^n + \lambda_{i-1}^+ a_i^- F_{i-1}^n - \left(\lambda_i^- a_i^- + \lambda_i^+ a_i^+\right) F_i^n\right], \quad (73)$$

$$F_i^{n+1} = \frac{c^2}{3\epsilon}\left[\left(\frac{a_i^+}{\lambda_i^+} + \frac{a_i^-}{\lambda_i^-}\right) E_i^n - \frac{a_i^+}{\lambda_i^+} E_{i+1}^n - \frac{a_i^-}{\lambda_i^-} E_{i-1}^n\right] + (1 - b_i) F_i^n - a_i^+ \frac{\lambda_{i+1}^-}{\lambda_i^+} F_{i+1}^n - a_i^- \frac{\lambda_{i-1}^+}{\lambda_i^-} F_{i-1}^n, \quad (74)$$

where

$$a_i^\pm = \frac{4\pi c \Delta t}{V_i \sqrt{3}} \frac{R_i^2 R_{i\pm1}^2}{\mp \frac{c\epsilon R_i^2}{\sqrt{3}\lambda_{i\pm1}^\mp} \pm \frac{c\epsilon R_{i\pm1}^2}{\sqrt{3}\lambda_i^\pm} + R_i^2 R_{i\pm1}^2 \epsilon \Delta f_{i\pm\frac{1}{2}}}, \quad (75)$$

$$b_i = -\left(\frac{cR_i^2}{\sqrt{3}R_{i+1}^2\lambda_{i+1}^-} - R_i^2 \Delta f_{i+\frac{1}{2}}\right)\frac{\sqrt{3}}{c}\lambda_i^+ a_i^+ - \left(\frac{cR_i^2}{\sqrt{3}R_{i-1}^2\lambda_{i-1}^+} + R_i^2 \Delta f_{i-\frac{1}{2}}\right)\frac{\sqrt{3}}{c}\lambda_i^- a_i^-, \quad (76)$$

$$\epsilon \Delta f_{i\pm\frac{1}{2}} = 4\sqrt{3}\,|R_{i\pm1} - R_i|\left(\frac{\sigma_s(R_{i\pm\frac{1}{2}})}{(R_i + R_{i\pm1})^2} + \frac{4\epsilon\mu_0\left(R_{i\pm\frac{1}{2}}\right)}{(R_i + R_{i\pm1})^3}\right). \quad (77)$$

Equality (70) is no more valid, but a similar relation holds:

$$b_i + a_i^+ + a_i^- = \frac{4\pi\Delta t}{V_i}\frac{R_i^2}{\epsilon}\left(\lambda_i^+ - \lambda_i^-\right).$$

Of course, if $\mu_0 = 0$, then $\lambda_i^\pm = \pm\frac{c}{\sqrt{3}}$, and (73)-(74)-(75)-(76)-(77) reduces to (65)-(66)-(67)-(68)-(69)-(70).

Lemma 3.6. *The scheme defined by* (73)-(74)-(75)-(76)-(77) *is* L^∞*-stable under the CFL condition*

$$a_i^\pm\left(1 - \frac{\lambda_i^\mp}{\lambda_i^\pm}\right) \leqslant \left|\lambda_i^\mp\right| \Delta t \frac{4\pi R_i^2}{\epsilon V_i} \leqslant 1. \quad (78)$$

Proof. In order to study the stability of the scheme, we write it with respect to the Riemann invariants

$$w_i^\pm = cE_i + \epsilon\frac{3}{c}\lambda_i^\mp F_i.$$

Using (73) and (74), a simple computation gives

$$w_i^{+,n+1} = \left(1 + \frac{4\pi\Delta t R_i^2}{\epsilon V_i}\lambda_i^-\right) w_i^{+,n} + \left(1 - \frac{\lambda_i^-}{\lambda_i^+}\right) a_i^+ w_{i+1}^{+,n} + \left(-\frac{4\pi\Delta t R_i^2}{\epsilon V_i}\lambda_i^- - \left(1 - \frac{\lambda_i^-}{\lambda_i^+}\right) a_i^+\right) w_i^{-,n},$$

$$w_i^{-,n+1} = \left(1 - \frac{4\pi\Delta t R_i^2}{\epsilon V_i}\lambda_i^+\right) w_i^{-,n} + \left(1 - \frac{\lambda_i^+}{\lambda_i^-}\right) a_i^- w_{i-1}^{-,n} + \left(\frac{4\pi\Delta t R_i^2}{\epsilon V_i}\lambda_i^+ - \left(1 - \frac{\lambda_i^+}{\lambda_i^-}\right) a_i^-\right) w_i^{+,n}.$$

The sum of the coefficients of each line is equal to 1. Hence, this system satisfies the maximum principle if and only if all coefficients are non-negative, that is,

$$1 \pm \frac{4\pi\Delta t R_i^2}{\epsilon V_i}\lambda_i^\mp \geqslant 0, \quad \mp\frac{4\pi\Delta t R_i^2}{\epsilon V_i}\lambda_i^\mp - \left(1 - \frac{\lambda_i^\mp}{\lambda_i^\pm}\right) a_i^\pm \geqslant 0,$$

which, using that $\lambda_i^- < 0 < \lambda_i^+$, is equivalent to (78). □

Remark 3.7. *In the case $\mu_0 = 0$, relation* (78) *simplifies into*

$$2a_i^\pm \leqslant \frac{c}{\sqrt{3}}\Delta t \frac{4\pi R_i^2}{\epsilon V_i} \leqslant 1.$$

As $\epsilon \to 0$, the coefficients $a_i^\pm$ are bounded, because $\epsilon\Delta f_{i\pm\frac{1}{2}}$ does not vanish. However, $\Delta t \dfrac{4\pi c R_i^2}{\epsilon V_i \sqrt{3}}$ behaves like ϵ^{-1}. More precisely, if ΔR is fixed and $\epsilon \to 0$, we have

$$a_i^\pm = \frac{\pi c \Delta t}{3 V_i \sigma_s(R_{i\pm\frac{1}{2}})\Delta R_{i\pm\frac{1}{2}}} \left(R_i + R_{i\pm1}\right)^2 + O(\epsilon). \tag{79}$$

On the other hand, a simple computation gives

$$V_i = \frac{4\pi}{3}\left[\left(R_i + \frac{\Delta R_i}{2}\right)^3 - \left(R_i - \frac{\Delta R_i}{2}\right)^3\right] = 4\pi R_i^2 \Delta R_i + \frac{\pi}{3}\Delta R_i^3 = 4\pi R_i^2 \Delta R_i + O(\Delta R^3). \tag{80}$$

Hence, using (79) and (80), the second condition in (78) gives, in the limit $\Delta R \to 0$,

$$\frac{c}{\sqrt{3}}\Delta t \leqslant \epsilon \Delta R + O(\Delta R^3).$$

In the case $\mu_0 \neq 0$, a similar analysis is possible, that gives

$$\left|\lambda_i^\pm\right| \Delta t \leqslant \epsilon \Delta R + O(\Delta R^3).$$

This condition is of hyperbolic type. However, when dealing with small values of ϵ, it proves very restrictive. A way to solve this difficulty is to make the scheme implicit. On the other hand, doing so, we need to solve, at each time step, a linear system. In order to avoid this, it is possible to make implicit only diagonal terms, as for instance in [17]. This is the aim of the next subsection.

3.3.3 Partially implicit Buet-Després type scheme

In this Section, we explain how one can obtain a stability condition that does not imply $\Delta t = 0$ when $\epsilon = 0$. For this purpose, we make implicit some of the terms of the scheme, which are stiff but diagonal. Hence the scheme can still be written as an explicit one.
Let us first do it in the case $\mu_0 = 0$. We replace (65)-(66) by

$$E_i^{n+1} = \left(1 - a_i^+ - a_i^-\right) E_i^n + a_i^+ E_{i+1}^n + a_i^- E_{i-1}^n + \frac{\epsilon\sqrt{3}}{c}\left[\left(a_i^- - a_i^+\right) F_i^n - a_i^+ F_{i+1}^n + a_i^- F_{i-1}^n\right], \quad (81)$$

$$(1+\delta_i)F_i^{n+1} = \frac{c}{\epsilon\sqrt{3}}\left[\left(a_i^+ - a_i^-\right) E_i^n - a_i^+ E_{i+1}^n + a_i^- E_{i-1}^n\right] + (1+\delta_i - b_i)F_i^n + a_i^+ F_{i+1}^n + a_i^- F_{i-1}^n. \quad (82)$$

where $\delta_i > 0$ is chosen in such a way that $1 + \delta_i - b_i$ is bounded as $\epsilon \to 0$. See (86) below for a "good" choice of δ_i. In the case of the P_1' model (that is, $\mu_0 \neq 0$), the same procedure gives the scheme

$$E_i^{n+1} = \left(1 - a_i^+ - a_i^-\right) E_i^n + a_i^+ E_{i+1}^n + a_i^- E_{i-1}^n + \frac{3\epsilon}{c^2}\left[\lambda_{i+1}^- a_i^+ F_{i+1}^n + \lambda_{i-1}^+ a_i^- F_{i-1}^n - \left(\lambda_i^- a_i^- + \lambda_i^+ a_i^+\right) F_i^n\right], \quad (83)$$

$$(1+\delta_i)F_i^{n+1} = \frac{c^2}{3\epsilon}\left[\left(\frac{a_i^+}{\lambda_i^+} + \frac{a_i^-}{\lambda_i^-}\right) E_i^n - \frac{a_i^+}{\lambda_i^+} E_{i+1}^n - \frac{a_i^-}{\lambda_i^-} E_{i-1}^n\right] + (1+\delta_i - b_i)F_i^n - a_i^+ \frac{\lambda_{i+1}^-}{\lambda_i^+} F_{i+1}^n - a_i^- \frac{\lambda_{i-1}^+}{\lambda_i^-} F_{i-1}^n \quad (84)$$

Lemma 3.8. *The scheme defined by* (83)-(84)-(75)-(76)-(77) *is* L^∞*-stable under the CFL condition*

$$\left(1 + \delta_i - \frac{\lambda_i^\mp}{\lambda_i^\pm}\right) a_i^\pm \leqslant \left|\lambda_i^\pm\right| \Delta t \frac{4\pi R_i^2}{\epsilon V_i} \leqslant 1 + \delta_i \left(1 - a_i^\mp\right). \quad (85)$$

Proof. As we did in the proof of Lemma 3.6, we write the scheme using the Riemann invariants $w^\pm$. We omit the details of the calculation, which is not difficult (although rather lengthy). We have

$$(1+\delta_i)w_i^{+,n+1} = \left(1 + \frac{4\pi\Delta t R_i^2}{\epsilon V_i}\lambda_i^- + \delta_i\left(1 - a_i^-\right)\right) w_i^{+,n} + \left(1 + \delta_i - \frac{\lambda_i^-}{\lambda_i^+}\right) a_i^+ w_{i+1}^{+,n} - \left(\frac{4\pi\Delta t R_i^2}{\epsilon V_i}\lambda_i^- + \left(1 + \delta_i - \frac{\lambda_i^-}{\lambda_i^+}\right) a_i^+\right) w_i^{-,n} + \delta_i a_i^- w_{i-1}^{-,n},$$

$$(1+\delta_i)w_i^{-,n+1} = \left(1 - \frac{4\pi\Delta t R_i^2}{\epsilon V_i}\lambda_i^+ + \delta_i\left(1 - a_i^+\right)\right) w_i^{-,n} + \left(1 + \delta_i - \frac{\lambda_i^+}{\lambda_i^-}\right) a_i^- w_{i-1}^{-,n} + \left(\frac{4\pi\Delta t R_i^2}{\epsilon V_i}\lambda_i^+ - \left(1 + \delta_i - \frac{\lambda_i^+}{\lambda_i^-}\right) a_i^-\right) w_i^{+,n} + \delta_i a_i^+ w_{i+1}^{+,n}.$$

One easily checks that in each line of the above scheme, the sum of the coefficients of the right-hand side is equal to $1+\delta_i$. Thus, a sufficient condition for stability is that all the coefficients are non-negative. Note that the conditions

$$1+\delta_i-\frac{\lambda_i^{\mp}}{\lambda_i^{\pm}}\geqslant 0 \text{ and } \delta_i a_i^{\pm}\geqslant 0$$

are always satisfied because $\delta_i\geqslant 0$, $a_i^{\pm}\geqslant 0$, $\lambda_i^{+}\geqslant 0$ and $\lambda_i^{-}\leqslant 0$. We are thus left with the conditions on the first and third coefficients of the right-hand side, which read

$$\left(1+\delta_i-\frac{\lambda_i^{\mp}}{\lambda_i^{\pm}}\right)a_i^{\pm}\leqslant \mp\frac{4\pi\Delta t R_i^2}{\epsilon_i}\lambda_i^{\mp}\leqslant 1+\delta_i\left(1-a_i^{\mp}\right).$$

These conditions are equivalent to (85). □

In order to choose δ_i, we impose that

1. the scheme remains consistent (we did not prove it yet, but we will do so in Proposition 3.9 below). This is achieved by imposing that $\delta_i=O(\Delta t)$ as $\Delta t\to 0$;
2. the stability condition (85) is not too severe as $\epsilon\to 0$. This is studied below

Another possible criterion is that the source terms appearing in (74) should be fully implicited. Hence, only the terms accounting for the numerical diffusion should remain. This is satisfied if

$$\delta_i=b_i+a_i^{+}\frac{\lambda_{i+1}^{-}}{\lambda_i^{+}}+a_i^{-}\frac{\lambda_{i-1}^{+}}{\lambda_i^{-}}. \tag{86}$$

Using this definition, we now analyze the stability constraints (85) as $\epsilon\to 0$. For this purpose, we recall that $a_i^{\pm}$ satifies (79), and that

$$\lambda_i^{\pm}=\pm\frac{c}{\sqrt{3}}+O(\epsilon), \tag{87}$$

as $\epsilon\to 0$. Inserting these estimates into (86), we infer

$$\delta_i=\frac{4\pi\Delta t}{\epsilon V_i}R_i^2\frac{2c}{\sqrt{3}}+O(1).$$

We then insert this, (79) and (87) into (85), which now reads

$$\frac{4\pi\Delta t}{\epsilon V_i}R_i^2\frac{2c}{\sqrt{3}}\,\frac{\pi c\Delta t}{3V_i\sigma_s(R_{i\pm\frac{1}{2}})\Delta R_{i\pm\frac{1}{2}}}\left(R_i+R_{i\pm 1}\right)^2\leqslant\frac{4\pi c\Delta t R_i^2}{\sqrt{3}\epsilon V_i}\leqslant\frac{4\pi\Delta t}{\epsilon V_i}R_i^2\frac{2c}{\sqrt{3}},$$

where we have discarded lower order terms. The second above inequality is always satisfied. The first one simplifies into

$$\frac{2\pi c\Delta t}{3V_i\sigma_s(R_{i\pm\frac{1}{2}})\Delta R_{i\pm\frac{1}{2}}}\left(R_i+R_{i\pm 1}\right)^2\leqslant 1.$$

This condition is of parabolic type. To see this, we assume now that $\Delta R_i\to 0$, and use (80), finding, up to higher order terms in ΔR_i,

$$\Delta t\leqslant\frac{3\sigma_s(R_{i\pm\frac{1}{2}})}{2c}\Delta R_i\Delta R_{i\pm\frac{1}{2}}.$$

The partially implicit scheme (83)-(84)-(75)-(76)-(77) is thus asymptotically stable in the sense of Defintion 3.3.

3.3.4 Theoretical study of the scheme

In this Section, we study the properties of the partially implicit Buet-Després type scheme (Section 3.3.3). We first study its behavior in terms of consistency. We then show that it preserves the stationary solutions up to the error of the quadrature on f_ϵ. Finally, we prove that it is asymptotic preserving when ϵ goes to 0.

Proposition 3.9. *Consider the partially implicit Buet-Després type scheme* (83)-(84)-(75)-(76)-(77) *associated with a trapezoidal quadrature for f_ϵ, with δ_i defined by* (86). *This scheme is first-order consistent in space and time with the P_1' model* (19).

Note that δ_i needs not be defined by (86). The proof we give below actually does not use (86), but only the fact that $\delta_i = O(\Delta t)$ as $\Delta t \to 0$.

Proof. For the sake of clarity, we assume that $\mu_0 = 0$ and that $\Delta R_i = \Delta R$ is constant. We first prove that the explicit scheme (65)-(66) is consistent.
First, (80) gives

$$V_i = 4\pi R_i^2 \Delta R + \frac{\pi}{3}\Delta R^3.$$

Next, we compute

$$\epsilon \Delta f_{i\pm\frac{1}{2}} = 4\sqrt{3}\sigma_s(R_{i\pm\frac{1}{2}})\frac{\Delta R}{(2R_i \pm \Delta R)^2} = \frac{\sqrt{3}\sigma_s(R_{i\pm\frac{1}{2}})}{R_i^2}\left(\Delta R \mp \frac{\Delta R^2}{R_i} + \frac{3}{4}\frac{\Delta R^3}{R_i^2} + O(\Delta R^4)\right).$$

Similarly, a simple computation gives

$$\frac{a_i^\pm}{\Delta t} = \frac{c}{2\epsilon\sqrt{3}\Delta R} + \frac{c}{2\epsilon\sqrt{3}}\left(\pm\frac{1}{R_i} - \frac{\sqrt{3}}{2\epsilon}\sigma_s(R_{i\pm\frac{1}{2}})\right) + O(\Delta R).$$

Hence, assuming that $R \mapsto \sigma_s(R)$ is of class C^1, we infer

$$\frac{a_i^+ + a_i^-}{\Delta t} = \frac{c}{\epsilon\sqrt{3}\Delta R} - \frac{c}{2\epsilon^2}\frac{\sigma_s(R_{i-\frac{1}{2}}) + \sigma_s(R_{i+\frac{1}{2}})}{2} + O(\Delta R) = \frac{c}{\epsilon\sqrt{3}\Delta R} - \frac{c\sigma_s(R_i)}{2\epsilon^2} + O(\Delta R).$$

Similarly,

$$\frac{a_i^+ - a_i^-}{\Delta t} = \frac{c}{\epsilon\sqrt{3}R_i} + \frac{c}{4\epsilon^2}\left(\sigma_s(R_{i-\frac{1}{2}}) - \sigma_s(R_{i+\frac{1}{2}})\right) + O(\Delta R) = \frac{c}{\epsilon\sqrt{3}R_i} + O(\Delta R).$$

Inserting these estimates in the first line of the scheme, we have

$$\begin{aligned}\frac{E_i^{n+1} - E_i^n}{\Delta t} &= \frac{a_i^+}{\Delta t}\left(E_{i+1}^n - E_i^n\right) - \frac{a_i^-}{\Delta t}\left(E_i^n - E_{i-1}^n\right) + \frac{\epsilon\sqrt{3}}{c\Delta t}\left[a_i^-\left(F_i^n + F_{i-1}^n\right) - a_i^+\left(F_i^n + F_{i+1}^n\right)\right] \\ &= \frac{a_i^+ - a_i^-}{\Delta t}\Delta R\partial_R E_i + \frac{\epsilon\sqrt{3}}{c\Delta t}2\left(a_i^- - a_i^+\right)F_i^n - \frac{\epsilon\sqrt{3}}{c\Delta t}\left(a_i^+ + a_i^-\right)\Delta R\partial_R F_i + O(\Delta R^2) \\ &= -\frac{2}{R_i}F_i^n - \frac{\epsilon\sqrt{3}}{c}\frac{c\Delta R}{\epsilon\sqrt{3}\Delta R}\partial_R F_i + O(\Delta R).\end{aligned}$$

This concludes the proof for the first equation. For the second one, a similar proof applies.

We have proved that the explicit scheme (65)-(66) is consistent. Then, it is an easy exercise to prove that the partially implicit scheme (81)-(82) is also consistent, noticing that

$$\delta_i = O(\Delta t) \text{ as } \Delta t \to 0.$$

The generalization of the above argument to $\mu_0 \neq 0$ and non-constant mesh size is tedious, but not conceptually difficult. □

Remark 3.10. *In Proposition 3.9, we have assumed that a trapezoidal quadrature is used for f. This is second-order consistent. If a rectangle method is used instead, it is first-order consistant, hence Proposition 3.9 still holds.*

We now deal with the way the scheme preserves the stationary solutions of the P_1' model. The derivation of the scheme from a conservative formulation is a good way to get a well-balanced scheme. However, the conservative variable is $\mathbf{W}$ which depends on an integral f_ϵ that is in general not computable. We show that the accuracy of the scheme on the stationary solutions is determined by the accuracy of the quadrature.

Proposition 3.11. *Let $p \in \mathbb{N}$ be the order of the space quadrature in the explicit Buet-Després type scheme* (73)-(74)-(75)-(76)-(77). *Then this scheme is well-balanced up to order p in space. The same conclusion holds for the partially implicit scheme* (83)-(84)-(75)-(76)-(77).

Proof. The stationary solutions of the P_1' model (19) are easily seen to be

$$E = C_2 - \frac{2\epsilon C_1 \mu_0(R)}{cR^2} - \frac{3C_1}{c}\int_{R_0}^{R} \frac{u\sigma_s(u)+2\epsilon\mu_0(u)}{u^3}du, \quad F_R = \frac{C_1}{R^2}, \tag{88}$$

for $C_1, C_2 \in \mathbb{R}$. A scheme is well-balanced (see Definition 3.1) if for an initial condition equal to a stationary solution,

$$E_i^{n+1} = E_i^n, \quad F_i^{n+1} = F_i^n, i, n \in \mathbb{N}.$$

This is equivalent to show that $\mathbf{W}_i^{n+1} = \mathbf{W}_i^n$ because the schemes on $\mathbf{U} = (cE/\sqrt{3}, F_R)$ and $\mathbf{W}$ only differ from a change of frame. Then, according to (61)-(62)-(63), it is sufficient to show that $\mathbf{Z}_{i+\frac{1}{2}}$ is independent of R. We know that $\mathbf{Z}_{i+\frac{1}{2}} = \phi(\mathbf{Z}_i, \mathbf{Z}_{i+1}, R_i, R_{i+1})$ for ϕ a given function that satisfies $\phi(\beta, \beta, R_i, R_{i+1}) = \beta$ for $\beta \in \mathbb{R}^2$. Hence, if $\mathbf{Z}_{i+\frac{1}{2}}$ is independent of R_i, R_{i+1}, the scheme is well-balanced. After inserting (88) in $\mathbf{Z}_i, \mathbf{Z}_{i+1}$, one computes

$$\mathbf{Z}_i = \left(\frac{cC_1}{\sqrt{3}}, c\left(\frac{cC_2}{3\epsilon} + \frac{C_1}{\sqrt{3}}\left(f_\epsilon(R_i) - \sqrt{3}\int_{R_0}^{R_i} \frac{s\sigma_s(s)+2\epsilon\mu_0(s)}{\epsilon s^3}ds\right)\right)\right).$$

Then if $f_\epsilon(R_i)$ is computed exactly, $\mathbf{Z}_i$ is independent of the radius vector R_i and the scheme is well-balanced. Otherwise the accuracy on the stationary solution is given by the error of the quadrature on f_ϵ. This concludes the proof for the explicit scheme. In the case of the partially implicit scheme, the same argument applies. □

We now focus on the asymptotic preserving property (in the sense of Definition 3.2) of the scheme.

Proposition 3.12. *The explicit Buet-Després type scheme* (73)-(74)-(75)-(76)-(77) *is asymptotically preserving in the sense of Definition 3.2. More precisely, as* ϵ *tends to* 0*, this scheme formally tends to the limit scheme*

$$\frac{E_i^{n+1}-E_i^n}{\Delta t}=\frac{\pi c}{V_i}\left(\frac{(R_i+R_{i+1})^2}{\Delta R_{i+\frac12}}\frac{E_{i+1}^n-E_i^n}{3\sigma_s(R_{i+\frac12})}-\frac{(R_i+R_{i-1})^2}{\Delta R_{i-\frac12}}\frac{E_i^n-E_{i-1}^n}{3\sigma_s(R_{i-\frac12})}\right). \tag{89}$$

This scheme is second order consistent in space and first order consistent in time with the diffusion equation

$$\partial_t E-\operatorname{div}\Big(\frac{c}{3\sigma_s}\nabla E\Big)=0. \tag{90}$$

The same result holds for the partially implicit scheme (83)-(84)-(75)-(76)-(77)*.*

Remark 3.13. *In Proposition 3.12, the trapezoidal method is used, ensuring a second-order consistency in space. If a first-order quadrature method is used, the limit scheme is no more* (89)*, and is only first order consistent. On the contrary, if a higher order quadrature method is used, then the limit scheme is given by* (89)*.*

Proof. The limit scheme can be obtained with a Chapman-Enskog expansion of E_i^n. We first note that, according to (75)-(76)-(77) on the one hand, and (18) on the other hand, $a_i^{\pm}$ and $\lambda_i^{\pm}$ satisfy (79) and (87), respectively, as $\epsilon\to 0$. Hence, the first equation of the scheme reads as

$$\begin{aligned}\frac{E_i^{n+1}-E_i^n}{\Delta t}=&\frac{\pi c\,(R_i+R_{i+1})^2}{3V_i\sigma_s(R_{i+\frac12})\Delta R_{i+\frac12}}\left(E_{i+1}^n-E_i^n\right)-\frac{\pi c\,(R_i+R_{i-1})^2}{3V_i\sigma_s(R_{i-\frac12})\Delta R_{i-\frac12}}\left(E_i^n-E_{i-1}^n\right)\\&+\frac{\epsilon\pi}{\sqrt{3}V_i}\left[\left(\frac{(R_i+R_{i-1})^2}{\sigma_s(R_{i-\frac12})\Delta R_{i-\frac12}}-\frac{(R_i+R_{i+1})^2}{\sigma_s(R_{i+\frac12})\Delta R_{i+\frac12}}\right)F_i^n\right.\\&\left.-\frac{(R_i+R_{i+1})^2}{\sigma_s(R_{i+\frac12})\Delta R_{i+\frac12}}F_{i+1}^n+\frac{(R_i+R_{i-1})^2}{\sigma_s(R_{i-\frac12})\Delta R_{i-\frac12}}F_{i-1}^n\right]+O(\epsilon).\end{aligned}$$

Hence,

$$\frac{E_i^{n+1}-E_i^n}{\Delta t}=\frac{\pi c\,(R_i+R_{i+1})^2}{3V_i\sigma_s(R_{i+\frac12})\Delta R_{i+\frac12}}\left(E_{i+1}^n-E_i^n\right)-\frac{\pi c\,(R_i+R_{i-1})^2}{3V_i\sigma_s(R_{i-\frac12})\Delta R_{i-\frac12}}\left(E_i^n-E_{i-1}^n\right)+O(\epsilon),$$

which converges to (89). To prove that this scheme is consistent with (90), we apply a finite volume scheme to (90), which gives

$$\partial_t E_i=\frac{c}{V_i}\left[\frac{S_{i+\frac12}}{3\sigma_s(R_{i+\frac12})}\frac{E_{i+1}-E_i}{\Delta R_{i+\frac12}}-\frac{S_{i-\frac12}}{3\sigma_s(R_{i-\frac12})}\frac{E_i-E_{i-1}}{\Delta R_{i-\frac12}}\right].$$

Pointing out that $S_{i\pm\frac12}=\pi\left(R_i+R_{i\pm1}\right)^2+O(\Delta R)$ and using an explicit time discretization, we recover (89). Here again, the argument was given for the explicit scheme, but carries over to the case of the partially implicit scheme. □

3.3.5 Numerical validations

In this Section, we validate numerically the previous theoretical properties: consistency, stability, accuracy on stationary solutions, asymptotic preserving property. Let us recall that the system under study is (19), and we use the partially implicit scheme (83)-(84), with (75)-(76)-(77).
Most test cases deal with domains excluding $R = 0$. We also present a test case including $R = 0$ both in transport and diffusion regimes. All the test cases are associated with a uniform mesh of space step ΔR. The two first test cases deal with the consistency of the scheme. For each test, boundary conditions are treated using ghost boundary cells.

3.3.5.1 Transient transport case. The first test case concentrates on the P_1 model corresponding to choose $\mu_0 = 0$ in the P_1' model. If σ_s is constant, it is possible to exhibit the following analytical solution:

$$\begin{cases} E(t,R) = \dfrac{K^{\frac{3}{2}}}{\epsilon R}\exp(t - R\sqrt{K}), \\ F_R(t,R) = \dfrac{RK + \sqrt{K}}{\epsilon R^2}\exp(t - R\sqrt{K}), \end{cases} \quad \text{with} \quad K = \frac{3(\epsilon^2 + c\sigma_s)}{c^2}. \tag{91}$$

The initial condition and the boundary condition are given by (91). Our parameters are chosen as:

- Domain: [1,2].
- $\Delta t = 10^{-5}$.
- $c = \epsilon = 1$.
- $\sigma_s(R) = 1$, $R \in [1, 2]$.
- $T_f = 1$ (final time).

On Figure 9, we plot the L^1 error on E and F_R for mesh steps ranging from $\Delta R = 10^{-5}$ to $\Delta R = 2 \times 10^{-2}$. We observe a first order consistency in space for E and F_R as expected.

3.3.5.2 A transparent-opaque case. The second test case validates the consistency in the case of the P_1' model with a domain containing the origin. In this test case we do not have an analytical solution. The domain $[0, 1.1]$ is composed of a transparent and a diffusive part $\sigma_s = \mathbb{1}_{0<R<1} + 10^3.\mathbb{1}_{1<R<1.1}$. We initialize the energy and the flux by

$$E(R) = \mathbb{1}_{R\leqslant 0.7}, \quad F_R(R) = 0.$$

We apply homogeneous Neumann boundary conditions at $R = 0$. At $R = 1.1$, we impose homogeneous Dirichlet conditions. The integral defining f_ϵ is approximated by a rectangle quadrature. We choose $\epsilon = c = 1$. We first compare the numerical solutions on E and F_R of the staggered scheme (in blue on Figures 10 and 11) to the Buet-Després scheme (in red on Figures 10 and 11) at $t = 0.5$ (Figure 10) and $t = 10$ (Figure 11). The discretization parameters are $\Delta R = 10^{-2}$ and $\Delta t = 10^{-4}$. The staggered scheme produces oscillations in the transparent domain for both times contrary to the partially implicit Buet-Després type scheme. In the opaque region, they both behave well.
Because there is no analytical solution, the reference solution is given by the partially implicit Buet-Després type scheme with a fine mesh: $\Delta R = 10^{-6}$. We plot the L^1 error on E and F_R obtained

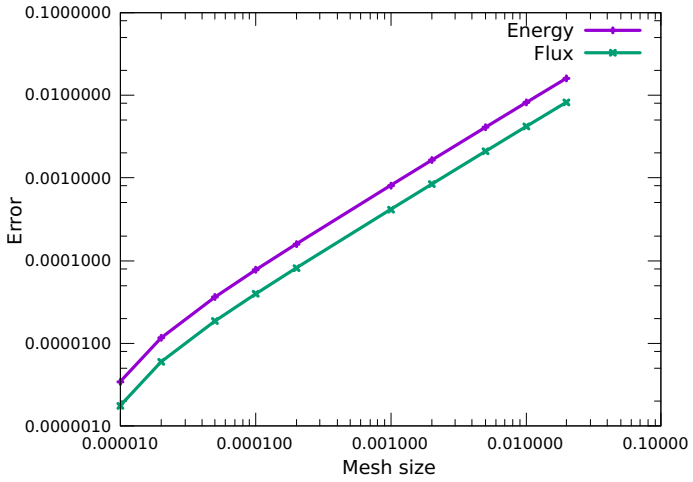

Figure 9: L^1 Error with respect to the mesh size ΔR for the transient transport case (91) of paragraph 3.3.5.1.

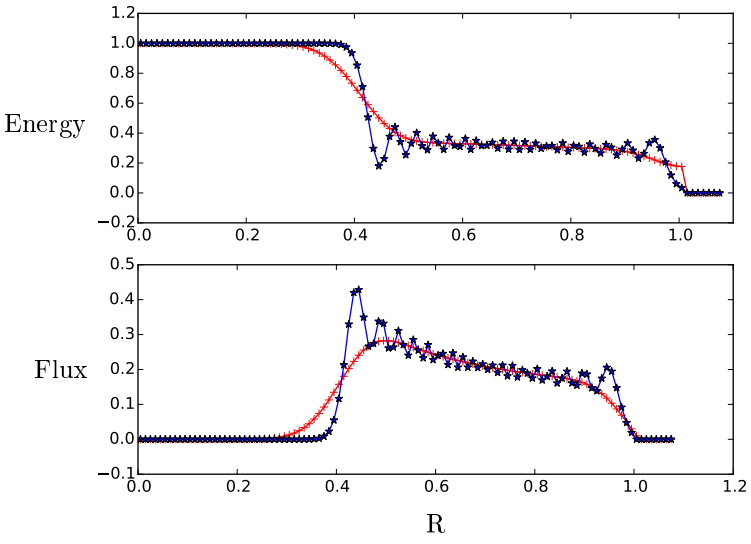

Figure 10: Comparison of the staggered scheme (blue) and the Buet-Després scheme (red) for the case described in paragraph 3.3.5.2, at time $t = 0.5$. Up: energy E as a function of R. Down: flux F_R as a function of R.

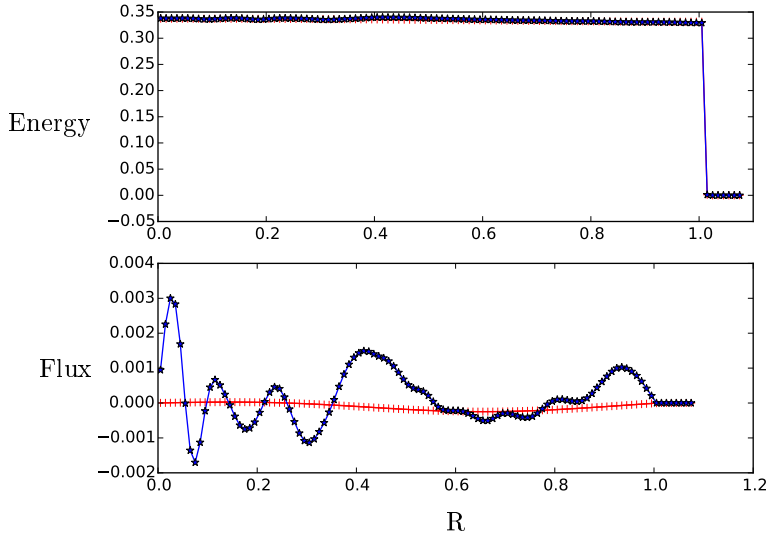

Figure 11: Comparison of the staggered scheme (blue) and the Buet-Després scheme (red) for the case described in paragraph 3.3.5.2, at time $t = 10$. Up: energy E as a function of R. Down: flux F_R as a function of R.

with the partially implicit Buet-Després type scheme for mesh steps ranging from $\Delta R = 10^{-5}$ to $\Delta R = 2 \times 10^{-2}$ (Figure 12). We choose the final time $T_f = 0.5$. We note that the method is first order convergent in space for both quantities.

3.3.5.3 Equilibrium states for P_1'. The third test case deals with the preservation of the stationary solution of the P_1' model, thereby validating Proposition 3.11. We recall that the P_1' model preserves the solution of the stationary radiative transfer equation in pure transport. According to Section 1.3, it is given by

$$E(R) = \frac{2\pi}{c}(1 + \mu_0(R)), \quad F_R(R) = -\frac{\pi R_1^2}{R^2}, \tag{92}$$

where R_1 is the radius of the inner sphere (Figure 5) and

$$\mu_0(R) = \mathbb{1}_{R>R_1}\sqrt{1 - \frac{R_1^2}{R^2}}. \tag{93}$$

We use (92) as the initial and boundary conditions. Our parameters are chosen as:

- Domain: $[1, 2]$, $R_1 = 1.25$.
- $\Delta t = 10^{-3}$, $\Delta R = 10^{-2}$.
- $c = \epsilon = 1$.

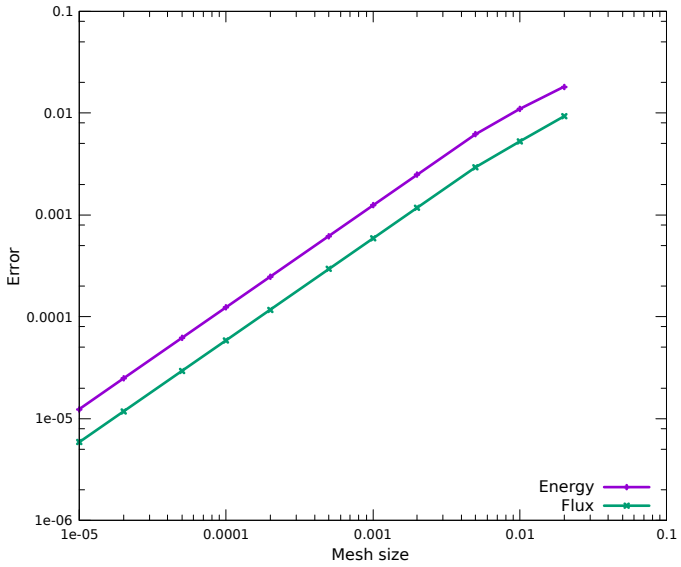

Figure 12: L^1 error for the transparent-opaque case (paragraph 3.3.5.2).

- $\sigma_s(R) = 0$, $R \in [1, 2]$.
- $T_f = 1$ (final time).

For this choice of parameters, f_ϵ is exactly computable: we expect this scheme to preserve exactly this stationary solution when no quadrature is considered. On Figure 13 the profiles of E and F_R are plotted. The blue curve corresponds to the initial condition and the red one to the scheme at time $t = T_f = 1$. On Figure 14, the relative error between the numerical approximation and the exact solution is plotted as a function of R. We note that the error is of the order of the machine epsilon.

3.3.5.4 Comparison of different quadrature methods for P_1'. This case is the same as the preceding one, but we consider three different quadratures for f_ϵ (the rectangle approximation, the trapezoidal approximation and the exact expression). In Proposition 3.11, a Taylor expansion is used, so we need f_ϵ to be smooth. This is why for the same domain we choose $R_1 = 0.75$: this moves the singularity of μ_0 out of the domain. Since we are only interested in the quadrature error, we choose the final time $T_f = 2.10^{-5}$ (that is, two time steps in the simulation), $\Delta t = 10^{-5}$ and ΔR ranges from $\Delta R = 10^{-5}$ to $\Delta R = 2 \times 10^{-2}$. We plot (Figure 15) the L^1 error on F_R as a function of the mesh size ΔR. The rectangle approximation is first order convergent, the trapezoidal approximation is second order convergent, and the analytical formula gives machine epsilon error, in concordance with Proposition 3.11.

3.3.5.5 Transient diffusion limit case. The last test case validates Proposition 3.12 about the asymptotic preserving property of the scheme. It also exhibits the parabolic stability condition

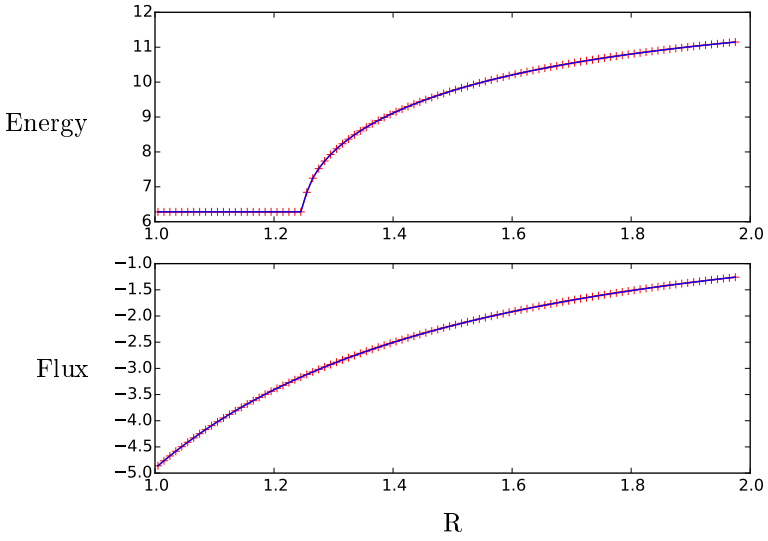

Figure 13: Stationary solution (92)-(93) (paragraph 3.3.5.3) for the P_1' model, computed with the Buet-Despres scheme.

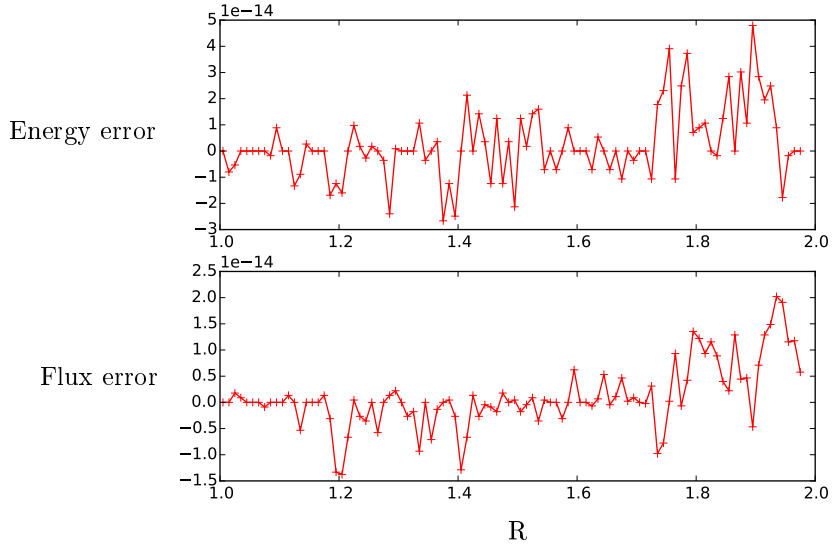

Figure 14: Relative error for the stationary solution (92)-(93) (paragraph 3.3.5.3) for the P_1' model, computed by the Buet-Despres scheme.

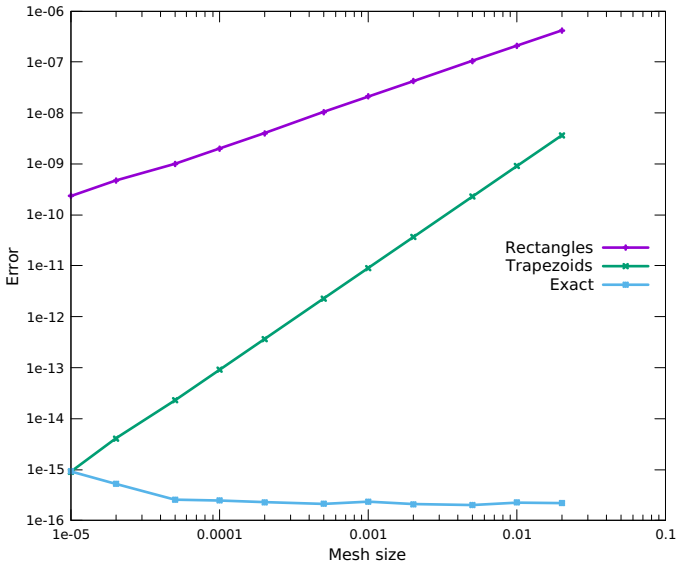

Figure 15: L^1 error on the flux F_R for different quadrature methods for the P_1' model in the case described in paragraph 3.3.5.4.

of the kind $\Delta t \leqslant \Delta R^2$ as ϵ goes to 0. To do so, we consider an exact solution of the diffusion equation ([17]) for $\sigma_s = 1$

$$E(t,R) = \frac{1}{R\sqrt{at}} \exp\left(-\frac{R^2}{4at}\right), \quad a = \frac{c}{3}, \quad t, R > 0. \tag{94}$$

Here the P_1' model for $\mu_0(R) = 1$ for all R is considered. Hence the function f_ϵ is computable analytically. The domain is $[0.1, 1]$. The initial condition is thus 0, and the boundary conditions are given by (94). Figure 16 shows the consistency with the diffusion equation in the limit $\epsilon \to 0$, according to the quadrature applied to f_ϵ (rectangle method, trapezoidal method, exact formula). We plot the L^1 error on E as a function of ΔR for a range of ΔR such that $\Delta t \leqslant \Delta R^2$ and for the parameters $c = 1$, $\epsilon = 10^{-12}$, $\Delta t = 10^{-8}$, $T_f = 10^{-6}$.

References

[1] Milton Abramowitz and Irene A. Stegun. *Handbook of mathematical functions with formulas, graphs, and mathematical tables*, volume 55 of *National Bureau of Standards Applied Mathematics Series*. For sale by the Superintendent of Documents, U.S. Government Printing Office, Washington, D.C., 1964.

[2] Christophe Berthon, Christophe Chalons, and Rodolphe Turpault. Asymptotic-preserving Godunov-type numerical schemes for hyperbolic systems with stiff and nonstiff relaxation terms. *Numer. Methods Partial Differential Equations*, 29(4):1149–1172, 2013.

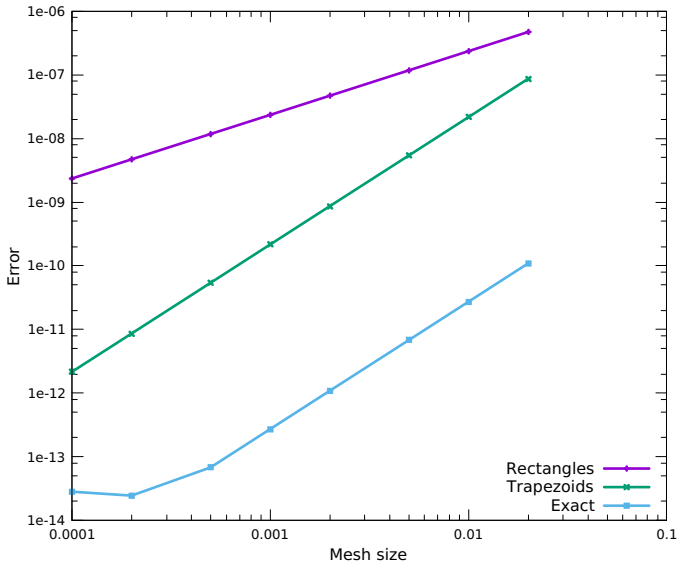

Figure 16: L^1 error on E as a function of ΔR for different quadratures, in the case described in paragraph 3.3.5.5.

[3] Christophe Berthon and Rodolphe Turpault. Asymptotic preserving HLL schemes. *Numer. Methods Partial Differential Equations*, 27(6):1396–1422, 2011.

[4] Thomas A. Brunner and James Paul Holloway. Two-dimensional time dependent Riemann solvers for neutron transport. *J. Comput. Phys.*, 210(1):386–399, 2005.

[5] Christophe Buet, Bruno Després, and Emmanuel Franck. Design of asymptotic preserving finite volume schemes for the hyperbolic heat equation on unstructured meshes. *Numer. Math.*, 122(2):227–278, 2012.

[6] Christophe Buet, Bruno Després, Emmanuel Franck, and Thomas Leroy. Proof of uniform convergence for a cell-centered AP discretization of the hyperbolic heat equation on general meshes. *Math. Comput.*, 86(305):1147–1202, 2017.

[7] John Castor. *Radiation Hydrodynamics.* Cambridge University Press, 2004.

[8] Subrahmanijan Chandrasekhar. *Radiative transfer.* Dover Publications, Inc., New York, 1950.

[9] Bruno Després and Christophe Buet. The structure of well-balanced schemes for Friedrichs systems with linear relaxation. *Applied Mathematics and Computation*, 272(2):440–459, 2016. Recent Advances in Numerical Methods for Hyperbolic Partial Differential Equations.

[10] Bruno Dubroca and Jean-Luc Feugeas. Étude théorique et numérique d'une hiérarchie de modèles aux moments pour le transfert radiatif. *C. R. Acad. Sci., Paris, Sér. I, Math.*, 329(10):915–920, 1999.

[11] Alan Robert Edmonds. *Angular momentum in quantum mechanics. Repr.* Princeton, NJ: Princeton Univ. Press, repr. edition, 1996.

[12] Alexandre Ern and Jean-Luc Guermond. Discontinuous Galerkin methods for Friedrichs' systems. In *Numerical mathematics and advanced applications. Proceedings of ENUMATH 2005, the 6th European conference on numerical mathematics and advanced applications, Santiago de Compostela, Spain, July 18–22, 2005.*, pages 79–96. Berlin: Springer, 2006.

[13] Alexandre Ern and Jean-Luc Guermond. Discontinuous Galerkin methods for Friedrichs' systems. I: General theory. *SIAM J. Numer. Anal.*, 44(2):753–778, 2006.

[14] Alexandre Ern and Jean-Luc Guermond. Discontinuous Galerkin methods for Friedrichs' systems. II: Second-order elliptic PDEs. *SIAM J. Numer. Anal.*, 44(6):2363–2388, 2006.

[15] Alexandre Ern and Jean-Luc Guermond. Discontinuous Galerkin methods for Friedrichs' systems. Part III. Multifield theories with partial coercivity. *SIAM J. Numer. Anal.*, 46(2):776–804, 2008.

[16] Joseph A. Fleck, Jr. and J. D. Cummings. An implicit Monte Carlo scheme for calculating time and frequency dependent nonlinear radiation transport. *J. Comput. Phys.*, 8:313–342, 1971.

[17] Emmanuel Franck. *Design and numerical analysis of asymptotic preserving schemes on unstructured meshes. Application to the linear transport and Friedrichs systems.* PhD thesis, Université Pierre et Marie Curie - Paris VI, October 2012.

[18] Kurt Otto Friedrichs. Symmetric positive linear differential equations. *Commun. Pure Appl. Math.*, 11:333–418, 1958.

[19] Matthias González, Neil M. H. Vaytet, Benoît Commerçon, and Jacques Masson. Multigroup radiation hydrodynamics with flux-limited diffusion and adaptive mesh refinement. *Astronomy and Astrophysics*, 578(A12), 2015.

[20] Laurent Gosse and Giuseppe Toscani. An asymptotic-preserving well-balanced scheme for the hyperbolic heat equations. *C. R. Math. Acad. Sci. Paris*, 334(4):337–342, 2002.

[21] James M. Greenberg and Alain-Yves Le Roux. A well-balanced scheme for the numerical processing of source terms in hyperbolic equations. *SIAM J. Numer. Anal.*, 33(1):1–16, 1996.

[22] Steven W. Haan. Radiative transport between concentric spheres. Technical report, Lawrence Livermore National Laboratory, 1994.

[23] Cory Hauck and Ryan McClarren. Positive P_N closures. *SIAM J. Sci. Comput.*, 32(5):2603–2626, 2010.

[24] Jingwei Hu, Shi Jin, and Qin Li. Asymptotic-preserving schemes for multiscale hyperbolic and kinetic equations. In *Handbook of numerical methods for hyperbolic problems*, volume 18 of *Handb. Numer. Anal.*, pages 103–129. Elsevier/North-Holland, Amsterdam, 2017.

[25] Shi Jin. Asymptotic preserving (AP) schemes for multiscale kinetic and hyperbolic equations: a review. *Lecture Notes for Summer School on "Methods and Models of Kinetic Theory" (M and MKT)*, 2010.

[26] Shi Jin. Asymptotic preserving (AP) schemes for multiscale kinetic and hyperbolic equations: a review. *Riv. Math. Univ. Parma (N.S.)*, 3(2):177–216, 2012.

[27] Shi Jin and C. David Levermore. Numerical schemes for hyperbolic conservation laws with stiff relaxation terms. *J. Comput. Phys.*, 126(2):449–467, 1996.

[28] Edward W. Larsen and Jim E. Morel. Asymptotic solutions of numerical transport problems in optically thick, diffusive regimes. II. *J. Comput. Phys.*, 83(1):212–236, 1989.

[29] C. David Levermore. Relating eddington factors to flux limiters. *J. Quant. Spectrosc. Radiat. Transfer*, 31(2):149 – 160, 1984.

[30] C. David Levermore. Moment closure hierarchies for kinetic theories. *J. Stat. Phys.*, 83(5-6):1021–1065, 1996.

[31] Iván Lux and Lázsló Koblinger. *Monte Carlo particle transport methods: neutron and photon calculations.* CRC Press, 1991.

[32] Ryan G. McClarren and Cory D. Hauck. Robust and accurate filtered spherical harmonics expansions for radiative transfer. *J. Comput. Phys.*, 229(16):5597–5614, 2010.

[33] Ryan G. Mcclarren, James Paul Holloway, and Thomas A. Brunner. A P1 benchmark for time dependent thermal radiative transfer, 2007.

[34] Ryan G. McClarren, James Paul Holloway, and Thomas A. Brunner. On solutions to the P_n equations for thermal radiative transfer. *J. Comput. Phys.*, 227(5):2864–2885, 2008.

[35] Bertrand Meltz. *Analyse mathématique et numérique de systèmes d'hydrodynamique compressible et de photonique en coordonnées polaires.* PhD thesis, Université Paris-Saclay, 2015.

[36] Dimitri Mihalas and Barbara Weibel Mihalas. Foundations of radiation hydrodynamics. New York etc.: Oxford University Press. XV, 718 p., 1984.

[37] Jim E. Morel, Todd A. Wareing, Robert B. Lowrie, and D. Kent Parsons. Analysis of ray-effect mitigation techniques. *Nuclear science and engineering*, 144(1):1–22, 2003.

[38] Frank W. J. Olver, Daniel W. Lozier, Ronald F. Boisvert, and Charles W. Clark, editors. *NIST handbook of mathematical functions.* Cambridge: Cambridge University Press, 2010.

[39] Gerald C. Pomraning. *Linear kinetic theory and particle transport in stochastic mixtures.* Singapore etc.: World Scientific, 1991.

[40] Jerome Spanier and Ely M. Gelbard. Monte Carlo principles and neutron transport problems. Addison-Wesley Series in Computer Science and Information Processing. Reading, Mass.-Menlo Park, Calif.-London-Don Mills, Ontario: Addison- Wesley Publishing Company. XIV, 234 p. 140 s (1969)., 1969.

[41] Rodolphe Turpault. A consistent multigroup model for radiative transfer and its underlying mean opacities. *J. Quant. Spectrosc. Radiat. Transfer*, 94(3):357–371, 2005.

[42] Wasaburo Unno and Masaaki Kondo. The eddington approximation generalized by radiative transfer in spherically symmetric systems. I. Basic methods. *Publ. Astron. Soc. Japan*, 28:347–354, 1976.

[43] Xavier Valentin. *Mathematical and numerical analysis of P_n models for photons transport problems.* Theses, Université Paris-Saclay, December 2015.

[44] Neil M. H. Vaytet, Edouard Audit, Bruno Dubroca, and Franck Delahaye. A numerical model for multigroup radiation hydrodynamics. *J. Quant. Spectrosc. Radiat. Transfer*, 112(8):1323 – 1335, 2011.